[American Journal of Science, Vol. 311, January, 2011, P. 27–62, DOI 10.2475/01.2011.02]

# TECTONIC SIGNIFICANCE OF DUCTILE DEFORMATION IN LOW-GRADE SANDSTONES IN THE MESOZOIC OTAGO SUBDUCTION WEDGE, NEW ZEALAND

JEFFREY M. RAHL*, MARK T. BRANDON**, HAGEN DECKERT***, UWE RING[§], and NICK MORTIMER[§§]

**ABSTRACT. This study demonstrates how ductile strain measurements can determine the tectonic evolution of a large and long-lived subduction wedge. We provide a synthesis of the geology of the South Island of New Zealand, with an emphasis on a wedge tectonics perspective that contrasts with a traditional view that interprets New Zealand geology in the context of terrane collision and accretion. We argue that the Otago subduction wedge evolved in a steady fashion throughout its 290 to 105 Ma history in response to accretion of trench-fill and abyssal-plain sediments, and slow erosion of a subaerially-exposed forearc high. Maximum temperatures for rocks in the flanks of the forearc high were no greater than 150 to 300 °C, with solution mass-transfer active as the dominant ductile mechanism. The 54 studied samples provide information about the absolute ductile strains acquired all along their flow-path, from the site of accretion to exhumation in the forearc high. We use tensor-averages to estimate strain at a regional scale. These show plane-strain uniaxial flattening, given that the tensor-averages for $S_y$ and $S_x$ are close to one. On average, $S_z$ is approximately 0.77, and this is balanced by a mass loss of about 23 percent. The average Z direction is sub-horizontal in the prowedge and moderately plunging in the retrowedge, a difference attributed to spatial variations in the mode of accretion. We infer that rocks presently in the pro-side of the Otago high were sourced by frontal accretion, and those in the retro-side were underplated. This result highlights the important role of accretion in determining the style of within-wedge deformation, and also demonstrates the benefit of using a tensor-averaging approach to examine regional strain.**

Key words: Subduction wedge, New Zealand, strain analysis, solution mass-transfer, Otago schist

## INTRODUCTION

The South Island of New Zealand exposes a well-known and well-preserved example of an ancient convergent margin. Of particular interest are the deformed and variably exhumed rocks in the forearc high region, which include multiply-folded, strongly-lineated schists with a generally flat-lying foliation (Mortimer, 1993a; Turnbull and others, 2001; Mortimer, 2003). There has been considerable debate regarding the origin of these fabrics and how they relate to the subduction history; models have related the fabrics to nappe stacking (Cox, 1991), terrane collision (Mortimer, 1993a), strong subduction shearing (Wood, 1978), or extensional collapse (Forster and Lister, 2003). Provenance studies suggest that units within this convergent margin may have been variably offset by strike-slip motion (Adams and others, 1998), raising the possibility that the fabrics formed during oblique subduction. The orientation of structures in the Otago region show regionally significant spatial variations (Mortimer, 1993a), so careful consideration is needed to understand how local measurements relate to kinematics at the regional scale.

* Department of Geology, Washington and Lee University, Lexington, Virginia, 24450 USA; RahlJ@wlu.edu
** Department of Geology and Geophysics, Yale University, P.O. Box 208109, New Haven, Connecticut, 06520-8109 USA
*** Institut für Geowissenschaften, Johannes Gutenberg-Universität, Becherweg 21, 55099 Mainz, Germany
§ Department of Geological Sciences, University of Canterbury, Christchurch, New Zealand
§§ GNS Science, Private Bag 1930, Dunedin, New Zealand

Our goal is to understand how the preserved fabric relates to the tectonic evolution of the Otago subduction wedge. In this contribution, we report 54 absolute strain measurements from sandstones exposed in low-grade flanks of the Otago forearc high. In contrast to previous studies that focused on relative strain measurements (Norris and Bishop, 1990; Stallard and others, 2005), our approach allows us to directly quantify the volume change component of the deformation. Although regional deformation is often assumed to be constant volume (isochoric), numerous studies suggest that regional-scale volume strains can be significant, particularly in low-grade settings, like Otago, where pressure solution is an important deformation mechanism (Ramsay and Wood, 1973; Wright and Platt, 1982; Wright and Henderson, 1992; Feehan and Brandon, 1999; Ring and Brandon, 1999; Ring and others, 2001; Richter and others, 2007). Ramsay and Wood (1973) were first to point out the shortcomings of relative strain data. In particular, they noted that oblate strains were commonly observed but given that volume strain was unknown, there was no way to know if this strain was due to flattening, constriction, or plane strain. Note that we prefer the term solution mass-transfer (SMT) over the more commonly used pressure solution because in detail there are a variety of processes, in addition to sensitivity of solubility to normal stress, that are associated with this deformation mechanism.

The absolute strain results presented here provide insight into the tectonic evolution of the Otago wedge and support several new interpretations, including: 1) the bulk regional deformation was approximately coaxial and nearly plane strain; 2) the well-developed lineations formed in the absence of significant regional tectonic extension; and 3) the pattern of deformation reflects the overall flux of material through the wedge, from accretion to exhumation. Our results highlight the advantages of using absolute strains and tensor averages for interpreting tectonic histories.

## TECTONIC SYNTHESIS

Australia, New Zealand, western Antarctica, and western South America collectively preserve evidence of a long-lived subduction zone active along the continental margin of eastern Gondwana from at least the late Paleozoic and persisting locally through today along the western margin of South America. New Zealand exposes a remarkable section, from arc to trench, across this eastern Gondwana subduction zone (Korsch and Wellman, 1988). Judging from the materials within the Otago wedge, accretion was active in the New Zealand sector from about 290 to 105 Ma, an interval of 195 Ma (Korsch and Wellman, 1988). The result was a ~450 km across-strike subduction wedge, comparable in size to the largest wedges observed today (for example, Makran >400 km; southeastern Alaska ~340 km; the Lesser Antilles ~325 km; Barbados ~325 km; Hellenic subduction wedge >400 km; Cascadia ~250 km). Exposures in the South Island represent only part of the wedge, which extends along strike for about 1500 km from the Chatham Islands to the west, through the Otago region, and continues on the western side of the Cenozoic Alpine fault in the central North Island. Unlike many wedges with mainly along-strike sections exposed, a long across-strike section outcrops throughout South Island.

In present coordinates, the downgoing slab was subducted to the southwest, with the magmatic arc (Median Batholith) located in the southwestern part of the South Island and the fossil trench located offshore to the north of the South Island (fig. 1). Numerical (for example, Willett and others, 1993; Burbidge and Braun, 2002) and analogue models (for example, Malavieille, 1984; Lallemand and others, 1994; Gutscher and others, 1998) suggest that many features of convergent margins like New Zealand are well-understood in the context of orogenic wedges (for example, Willett and others, 1993; Brandon, 2004; Fuller and others, 2006). These models indicate that at subduction zones accreted material is deformed into an asymmetric doubly-vergent wedge.

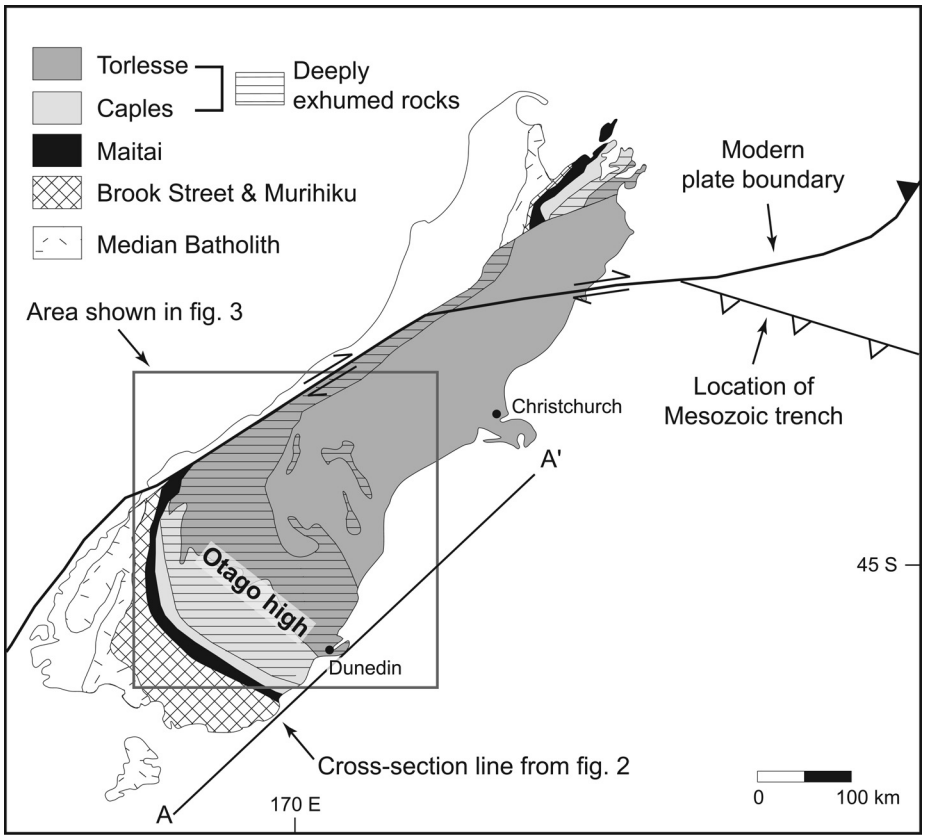


Fig. 1. Simplified geologic map of the pre-Cretaceous basement of the South Island, New Zealand (after Mortimer and others, 1999b).

This framework is useful for interpreting the geology of the South Island of New Zealand, a region characterized by a series of distinct lithostratigraphic units (figs. 1 and 2). To the southwest is the Median Batholith, a magmatic arc that initiated in the Carboniferous (~350 Ma) and remained active throughout the Early Cretaceous

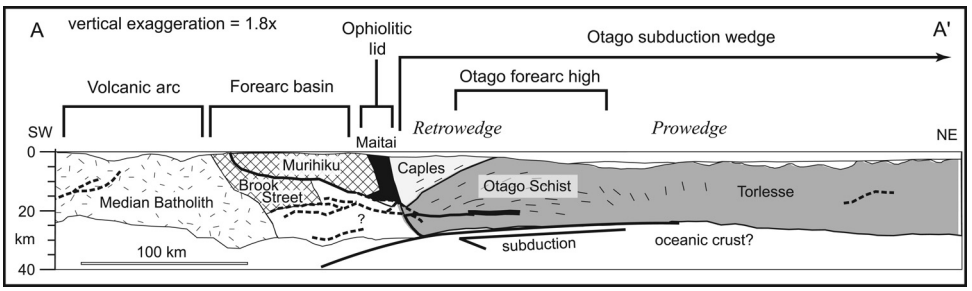


Fig. 2. Interpretative cross-section of the South Island, based on a crustal seismic reflection profile presented by Mortimer and others (2002). Heavy lines show interpreted faults; short lines represent schist foliation, which is horizontal beneath the Otago high and dips away to the NE and SW.

(~110 Ma), indicating semi-continuous convergence and subduction for nearly 250 Ma (Mortimer and others, 1999a, 1999b). In the South Island, the adjacent forearc region represents a structural lid, the tapered leading edge of the overriding plate prior to subduction (for example, Brandon, 2004). The structural lid is composed of three distinct lithologic terranes, which, from southwest to northeast, are the Brook Street, the Murihiku, and the Maitai. The Brook Street is dominated by Permian lavas and volcaniclastic sediments interpreted as a low-latitude intra-oceanic island arc and basin complex (for example, Haston and others, 1989). The Murihiku terrane is composed of volcaniclastic sandstones and mudstones interlayered with tuffs and is thought to represent a Permian to Jurassic forearc basin (Campbell and others, 2001). Farther outboard, the Permian to early Triassic Maitai terrane has two dominant assemblages: a mafic-ultramafic igneous complex (the Dun Mountain Ophiolite belt) and an overlying depositional sequence of graywacke and mudstone (Coombs and others, 1976). These represent a more outboard part of the forearc, with the Dun Mountain belt preserving part of the basement on which the overlying Maitai forearc basin was deposited. Together, these three lithostratigraphic units are distinct from the more outboard subduction complex in that they were always part of the overriding plate. These units were thrust over the more frontal part of the wedge by the Livingstone Fault, a steeply dipping zone of mélange up to a km thick that was subsequently overturned.

Outboard of the structural lid, the subduction complex is comprised of two large units, the Caples and Torlesse, that formed by accretion along the Otago subduction zone. The more inboard Caples is positioned within the retrowedge and is composed primarily of Permian and Triassic graywacke and mudstone derived from an immature island arc source. Farther outboard in the prowedge lies the Permian to Early Cretaceous graywacke and mudstone of the Torlesse supergroup, composed of the Rakaia (Permian to Late Triassic) and Pahau (Upper Jurassic to Early Cretaceous). Compared to the Caples, the dominantly quartzofeldspathic Torlesse sediments show affinities with a more evolved continental source (MacKinnon, 1983; Mortimer and Roser, 1992; Adams and others, 1998; Wandres and others, 2004a). Progressive accretion of the Torlesse is indicated by the younging of sediments towards the toe of the wedge (MacKinnon, 1983), based on sparse fossils.

Although the similarities between the Mesozoic geology of New Zealand and other convergent margins are widely recognized (MacKinnon, 1983), there has been substantial debate over the role of margin-parallel offsets between the various parts of the Gondwanan margin. Plate reconstructions (for example, Sutherland and Hollis, 2001) and sedimentary provenance analyses have been used to argue for substantial right-lateral (for example, Adams and others, 1998) or left-lateral (Wandres and others, 2004a) translation.

The early history of the wedge is complicated by the inferred margin-parallel translations. However, both the age of the sediments and the history of activity in the Median Batholith reach back to the Permian, so the Otago wedge may have been active since at least that time. Kear and Mortimer (2003) show that the Late Jurassic sediments of the Waipa Supergroup overlap the units of the Gondwanan margin, confirming that by this time all components of the margin were assembled in approximately their current geometry (Mortimer and others, 2002). We return to translation issue below because our results suggest the Caples preserves a minor amount of left-lateral shear.

The boundary between the Caples and Torlesse rocks lies within the Otago culmination, a 150 km wide structural arch oriented parallel to the strike of the ancient margin (Wood, 1978). The culmination represents the forearc high of the subduction wedge and exposes the most deeply exhumed and intensely metamorphosed and

deformed rocks in the region, referred to as the Otago Schist. Several lines of evidence indicate that slow erosion of an emergent forearc high was a persistent feature throughout the history of the Otago wedge. First, stratigraphic evidence preserves a long record of terrestrial deposition and subaerial exposure, with Middle Triassic plant material deposited by ~240 Ma (MacKinnon, 1983), the recycling of older Torlesse rocks into the Upper Jurassic to Early Cretaceous younger Torlesse (MacKinnon, 1983; Wandres and others, 2004b), and the incorporation of schistose clasts deposited in rift-related grabens at 102 Ma (Bishop and Laird, 1976; Adams and Raine, 1988). Second, the exhumation history for high-grade rocks in the high (discussed below) is consistent with slow but steady erosion throughout the history of the wedge. Finally, our strain results (presented below) show that within-wedge deformation lacked extension, indicating that erosion was responsible for exhumation of the high-grade rocks in the Otago culmination. We note that a deeply exhumed forearc high is a feature common to many modern subduction zones, including Cascadia (the Olympics) (Brandon, 2004), the Hellenic subduction zone (Crete) (Rahl and others, 2005), and southeastern Alaska (Kodiak Island) (Clendenen and others, 2003).

Metamorphism and deformation in the Otago region has often been interpreted in the context of discrete orogenic episodes caused by the docking of tectonic terranes. For example, the Rangitata orogen (Coombs and others, 1976; Wood, 1978; Mortimer, 1993a) was an inferred Mesozoic collision in which the Caples was thrust above the incoming Torlesse unit, creating the Otago Schist. A range of ages have been proposed for this "event," including Early Jurassic (for example, Adams and others, 1985), Middle Jurassic (Little and others, 1999), and Late Jurassic (Coombs and others, 1976; Gray and Foster, 2004). In contrast, we regard metamorphism and deformation as developing in a steady fashion during convergence on the Gondwanan margin. The nearly continuous record of arc magmatism and progressive younging of sediments towards the toe of the Otago wedge both suggest a gradual evolution instead of discrete orogenic episodes. The observed pattern of more intense metamorphism and deformation in a margin-parallel belt flanked by less disturbed rocks is a common feature of many active convergent wedges that grow through steady accretion (Willett and Brandon, 2002), reflecting a greater level exhumation due to focused erosion at the forearc high.

Metamorphic grade increases from the flanks towards the axis of the Otago Schist. Apatite fission-track ages are reset even in the lowest grade rocks of the Torlesse, indicating that all currently exposed rocks experienced temperatures in excess of 110 °C (Kamp, 1986). As noted by Vry and others (2008), estimation of peak metamorphic conditions for the monotonous grayschists of the Otago wedge is challenging due to mineral assemblages unsuitable for traditional thermobarometry. Furthermore, because plagioclase is consistently albite, geobarometers based on the partitioning of Ca between garnet and plagioclase are inapplicable. As an alternative, Vry and others (2008) present pseudosections for chemical compositions typical for the grayschists of the South Island. These pseudosections describe distinctive assemblages that can place constraints on the P-T conditions of the Otago rocks. Mortimer (2000) documents more than 15 localities from the high-grade rocks of eastern and central Otago with an assemblage of garnet + biotite + quartz + albite + phengite + chlorite + epidote. Vry and others (2008) show that the stability of this assemblage is largely governed by the abundance of Mn, which tends to stabilize garnet over a broad range of conditions. We focus on sample P50723 described by Little and others (1999) from near Hindon in eastern Otago. This sample contains the above mineral assemblage and has a Mn content of 0.03 percent (Mortimer, 2000); for this Mn concentration, the pseudosections of Vry and others (2008) show that the above mineral assemblage is stable over a narrow range of conditions, from 0.6 to 0.9 GPa and ~470 to 500 °C.

Another approach to estimating maximum pressures in the Otago rocks comes from the Si in phengite barometer (Massonne and Szpurka, 1997). Phengite from sample P50723 has a Si content of 3.3 to 3.4 per 11 oxygens. Given a temperature of about 500 °C, consistent with both the value from the pseudosections of Vry and others (2008) as well as a ~470 °C estimate from eastern Otago based on Raman spectroscopy of carbonaceous material reported by Rahl and others (2005), application of the Massonne and Szpurka (1997) calibration gives a pressure estimate of about 0.72 ± 0.08 GPa. Thus, both the pseudosection and phengite barometry approaches yield similar estimates, and we consider the maximum metamorphic conditions in the Otago culmination to be about 0.75 GPa and 500 °C. Assuming an average crustal density of 2750 kg $m^{-3}$, these pressures indicate a depth of about 27 km, consistent with estimates of crustal thickness based seismic data (Mortimer and others, 2002).

Clear establishment of the timing of metamorphism and exhumation has been difficult, in part because of uncertainty over whether white mica Ar ages represent cooling or crystallization. Recent $^{40}Ar/^{39}Ar$ work (Little and others, 1999; Forster and Lister, 2003; Gray and Foster, 2004) demonstrates an inverse correlation between white mica age and structural depth (Mortimer, 2003). Little and others (1999) model the cooling age/depth relationship and conclude that the Otago rocks experienced a time-varying cooling history, with a period of slow cooling from 180 to 135 Ma followed by a pulse of more rapid exhumation. However, this modeling approach assumes uniform erosion rates across the Otago wedge, and as noted above, spatial variations in exhumation rate perpendicular to strike are characteristic of mountain belts focused erosion on the core of a range (Brandon and others, 1998; Gasparini and Brandon, in review[1]).

To estimate the steady exhumation rate in the wedge, we apply a 1D thermal model that determines the best-fit thermal profile consistent with observed metamorphic and cooling age data (Reiners and Brandon, 2006). Although horizontal advection of rock and heat may bias estimates of exhumation based on 1D thermal models, these effects are minimized as rock particle paths become more vertical (Batt and Brandon, 2002). Vertical particle paths are favored when accretion occurs through underplating, a process our new strain data suggests is important in the Otago wedge. Therefore, we conclude the 1D thermal model applied here will provide a reasonable estimate of the steady exhumation rate. We focus on Little and others (1999) sample P50723 discussed above. They describe a white mica Ar age from this sample with a broad plateau age of 131.0 ± 1.3 Ma that may be interpreted to record cooling rather than crystallization given the metamorphic constraints discussed above. Model input parameters include a maximum T = 495 ± 10 °C; P = 0.72 ± 0.08 GPa; initial depth = 26.7 ± 3 km; and surface temperature of 10 °C based on high latitude Albian mean annual temperatures reported by Miller and others (2006). Sediments of the nearby Shag Point Group (fig. 3) contain conglomerates with clasts of high-grade Otago Schist. Zircon U-Pb ages of 112.3 ± 0.4 Ma from a tuff from the base of unit provides a constraint on the time of surface exposure of the Otago rocks (Tulloch and others, 2009). Given these inputs, the model (fig. 4) estimates a steady exhumation rate of ~1.00 mm/a, and a time of peak metamorphism of 144 Ma. Although this calculation is based upon a single well-studied sample, the overall similarity in Ar ages (for example, Gray and Foster, 2004) and metamorphic assemblages (Mortimer, 2000) along the strike of the Otago culmination suggests it is representative of the entire wedge. The calculated 1 mm/a rate is typical for erosion in active mountain belts, although higher rates (up to 10 mm/a) have been locally observed in some settings (Ring and others, 1999).

[1] Gasparini, N. M., and Brandon, M. T., in review, A power-law scaling relationship for bedrock incision at the drainage network scale: Journal of Geophysical Research—Earth Surface.

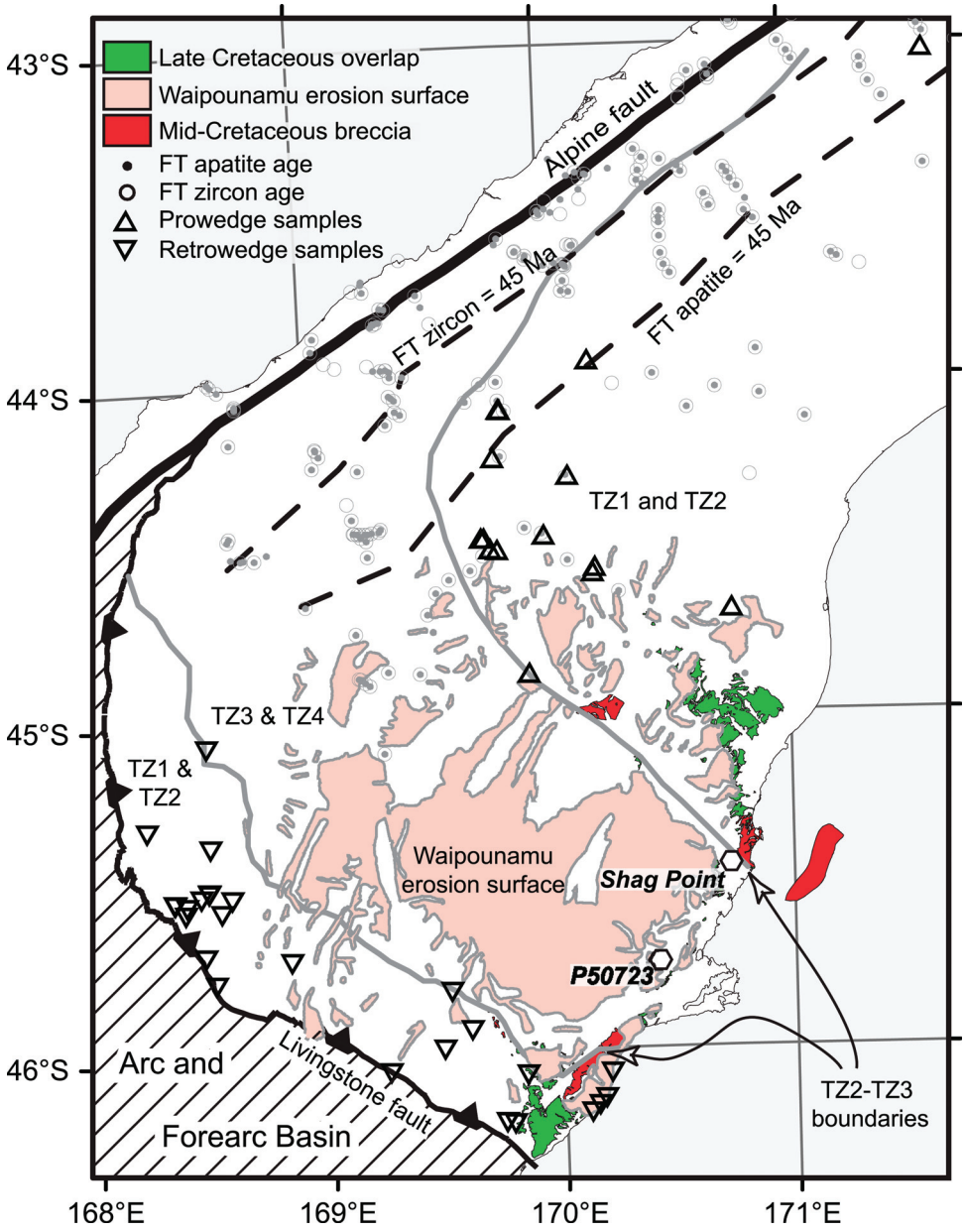


Fig. 3. Map showing key age constraints on the development of the Otago wedge. Young apatite and zircon fission-track ages (gray symbols) indicating Cenozoic cooling are confined to a zone near the Alpine Fault (data from Kamp and others, 1989; Tippett and Kamp, 1993; Kamp, 2001). The 45 Ma contour showing the eastern limit of Alpine exhumation are plotted. Note that none of our strain samples come from areas affected by substantial Alpine deformation. Also shown is the extent of the Waiponoamu erosion surface, mid-Cretaceous rift related breccias, and Late Cretaceous overlap sediments (Mortimer, 1993b).

Within-wedge deformation is well-preserved in the Otago Schist. Mélange is rare in the Caples and Torlesse (Nelson, 1982) and most units retain their original stratigraphic coherence at the outcrop scale. Accretionary thrust faults in the higher-

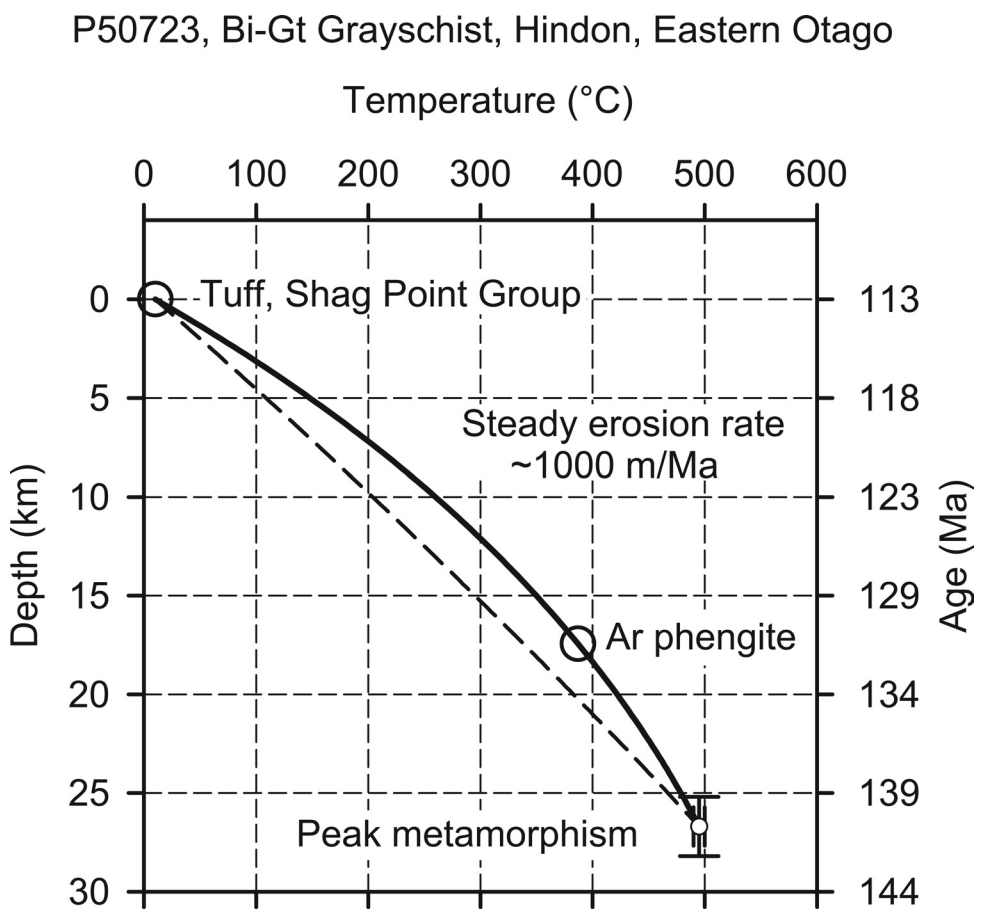


Fig. 4. Exhumation history calculated for a sample of high-grade schist from eastern Otago (Little and others, 1999) using a 1D thermal model (Reiners and Brandon, 2006). Solid line shows the best-fit exhumation history, consistent with steady erosion at a rate of 1000 m/Ma. The dashed line shows the calculated geothermal gradient assuming no upward heat advection due to erosion.

grade rocks are generally obscured by later metamorphism and deformation, though such structures are mapped in lower-grade rocks (Forsyth, 2001; Cox and Barrell, 2007). The oldest units are at the structurally highest position in the rear of the wedge, with progressively younger units present towards the toe (MacKinnon, 1983). Although greenstones, quartzites, and conglomerates are locally present, the bulk of the Otago wedge is composed of lithologically monotonous graywackes and mudstone. The lack of distinctive marker horizons impedes the identification of the regional structure. To overcome these difficulties, many workers have used a system of four textural zones (TZ1 to TZ4), originally described by Hutton and Turner (1936) and Bishop (1972) and redefined on the basis of white mica grain size and the degree of foliation development in the schist (Turnbull and others, 2001). The textural zones roughly correlate with structural depth (Mortimer, 2003), deformation (Norris and Bishop, 1990; Stallard and Shelley, 2005; Stallard and others, 2005), and metamorphic grade (Mortimer, 2000). Norris and Bishop (1990) reported that SMT was the sole ductile mechanism in TZ1 to TZ2A, but in TZ2B and higher rocks, dislocation glide and climb (DGC) was activated as a competing ductile mechanism. A penetrative

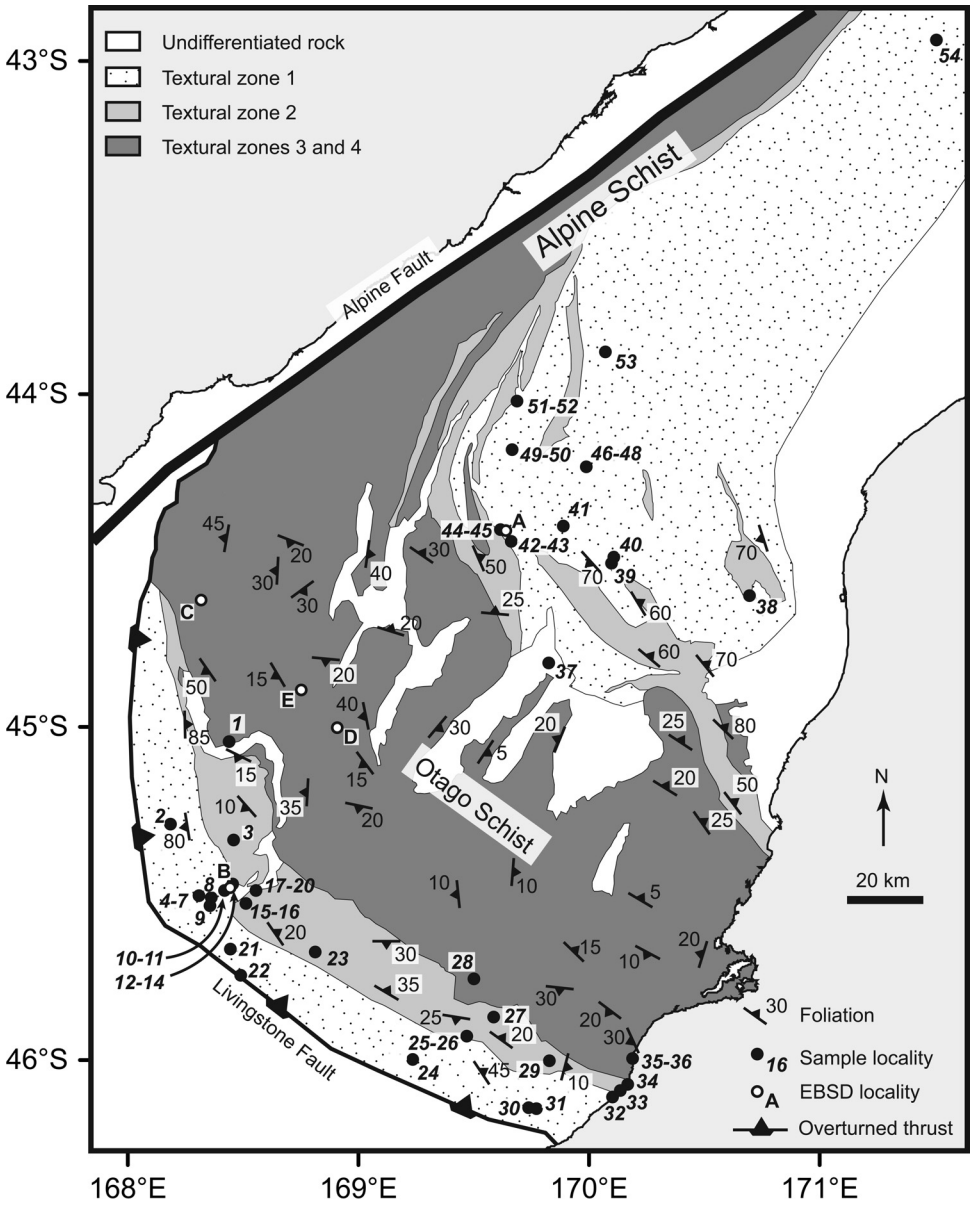


Fig. 5. Map of the study area. Sample localities are indicated by the black circles with bold italic numbers. The orientation of dominant foliation is shown after Mortimer (1993a).

foliation is subhorizontal in the core of the culmination, where strains are highest and the exhumation is greatest (figs. 2 and 5). This foliation progressively steepens towards the flanks of the culmination. A prominent mesoscopic lineation is commonly observed, defined by "quartz rodding." Although consistently oriented on a local scale, the direction of this lineation varies widely across the region (Mortimer, 1993a) (fig. 6).

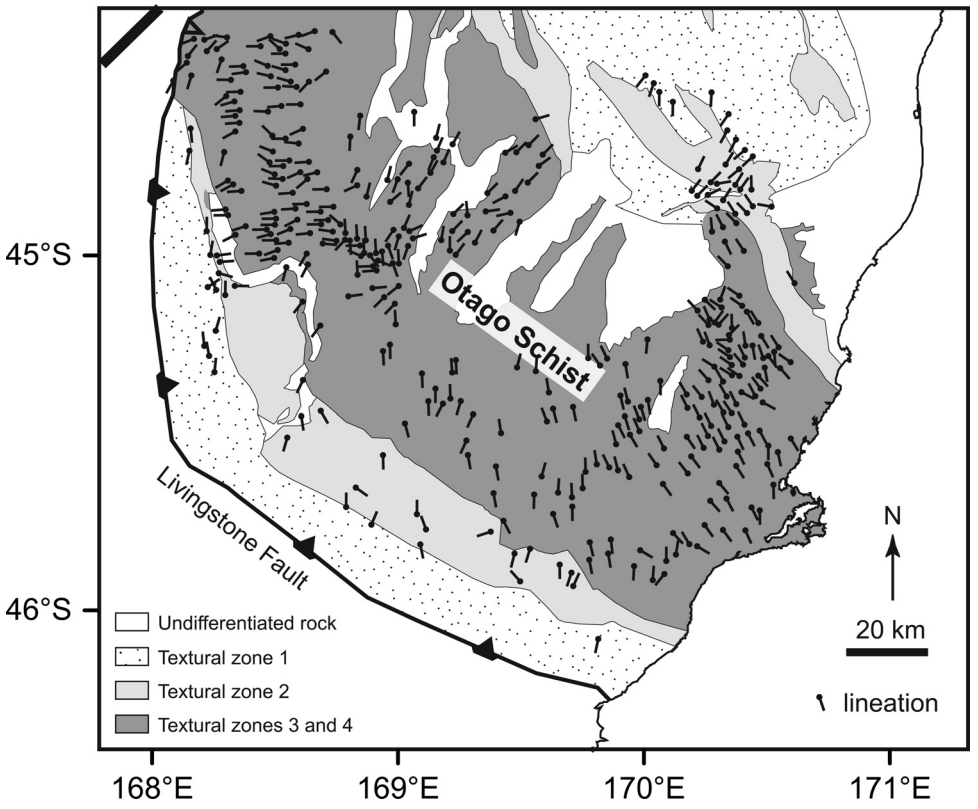


Fig. 6. Map of study area showing the azimuth of stretching lineations from Mortimer (1993a). The dots indicate the location of measurement. The data are not corrected for tilt, but because the foliation is generally shallow this does change the angular relationships significantly. Note the widely varying orientation throughout the region.

A fundamental question is what processes controlled deformation in the Otago wedge, and as noted above, several hypotheses have been proposed. As noted above, one popular view is that fabrics developed during orogenic episodes caused by the collision of tectonic terranes. A second idea is supported by recent work that has documented extensional shear zones in the Otago high (Deckert and others, 2002a; Forster and Lister, 2003). Deckert and others (2002a) suggest these features might be related to either 1) syn-convergent within-wedge extension, with basal accretion destabilizing the upper levels of the wedge (Platt, 1986), or 2) post-convergence rifting associated with the late-Cretaceous break-up of the Gondwanan margin. The recognition of normal-sense shear zones raises the question as to how the high-grade rocks of the forearc high were exhumed. We concur with Deckert and others (2002a) and believe the extensional deformation is related to the break-up of Gondwana, given that $Ar^{40}/Ar^{39}$ white mica cooling ages around 115 to 110 Ma (Forster and Lister, 2003; Gray and Foster, 2004) indicate these structures initiated contemporaneously with the onset of the rifting widely observed throughout New Zealand in Late Cretaceous time (Laird and Bradshaw, 2004). Furthermore, as described above, we argue that an eroding forearc high was a persistent feature throughout the history of the Otago wedge. For these reasons, we adopt an alternative view and consider the ductile features in Otago to reflect progressive deformation acquired during the full ~185 Ma history of the Otago wedge.

Convergence along the Gondwanan margin operated until about 105 Ma, when either the collision of a spreading ridge (Bradshaw, 1989), stalling of the downgoing slab (Luyendyk, 1995), or collision of the Hikurangi Oceanic Plateau (Mortimer, 2004) led to the cessation of subduction. Adakitic melts dominated the Median Batholith from 130 Ma until magmatism shut off at 105 Ma (Mortimer and others, 1999b), supporting the interpretation that subduction of young, hot oceanic crust contributed to the end of convergence. The youngest sediments in the Torlesse contain detrital zircons with 110 Ma fission-track ages that indicate accretion continued until at least that time (Wandres and others, 2004b). Although metamorphic mineral growth from the Alpine Schist has been cited as evidence that subduction continued until about 87 Ma (for example, Vry and others, 2004), we note that the widespread Late Cretaceous extension would advect isotherms towards the surface, driving new metamorphic mineral growth.

The Waipounamu erosion surface (WES) is a well-known low-relief upland surface recognized throughout the Otago region (Bishop, 1994; LeMasurier and Landis, 1996) (fig. 3). We envision that this surface may be a vestige of the eroded forearc high that persisted throughout the evolution of the wedge. Late Cretaceous (~87-86 Ma) sediments in eastern New Zealand and the offshore overlap the WES and demonstrate that the Otago wedge was not greatly dismembered during the Cretaceous extension that ultimately led to the opening of the Tasman Sea by 85 Ma (Adams and Raine, 1988; Korsch and Wellman, 1988; Laird and Bradshaw, 2004) (fig. 3). Gently folded remnants of the WES demonstrate that the region has experienced only mild deformation since the late Cretaceous related to the modern plate tectonic setting (Jackson and others, 1996).

Although most of the Otago wedge is relatively undisturbed by post-Cretaceous deformation, the western part of the study area has been affected by distributed shearing along the modern Alpine Fault since 45 Ma (Molnar and others, 1975; Sutherland, 1999). The lithostratigraphic units of the South Island show right-lateral shearing in a zone that extends >100 km on either side of the fault (for example, Little and Mortimer, 2001). Alpine deformation has also led to uplift and deep exhumation near the Alpine Fault. For example, published apatite fission-track ages are young and reset near the fault, in contrast to older ages preserved throughout the rest of the wedge (fig. 3) (Kamp, 2000). In our study, the bulk of our samples are collected away from the area affected by Cenozoic deformation, and we correct for post-wedge rotations below.

The synthesis described here highlights several reasons why the South Island of New Zealand is an ideal setting to study ductile deformation within a wedge: 1) plate tectonic, magmatic, and structural data all suggest that the Otago wedge experienced a long and relatively steady evolution; 2) wedge material advected from the site of accretion though the wedge, acquiring an integrated history of within-wedge deformation; 3) the presence of WES over most of the study region indicates that the wedge deformation history is relatively undisturbed, and lithospheric bending associated with recent Alpine deformation can be easily reconstructed.

## FIELD AND MICROSTRUCTURAL OBSERVATIONS

Our study is focused on measurements of absolute strains for 54 samples of TZ1 and TZ2A sandstones from the Caples and Torlesse units exposed in the flanks of the Otago culmination (fig. 5), where SMT is the dominant ductile deformation mechanism. We provide a brief description of the sampled region, including the local geology and microstructural changes observed with increasing textural zones.

In the field, the Caples and Torlesse are dominated by coherent sequences of thick and massive turbiditic sandstones with minor intercalated mudstone layers. Exotic lithologies, such as basalt, limestone, and chert, are present but rare. As

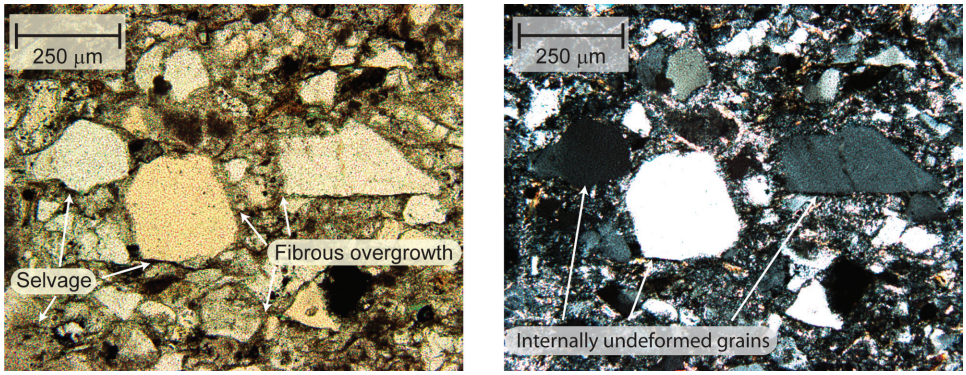


Fig. 7. Plane and polarized light images from sample 000303-4 illustrating the microstructures of the Otago Schist rocks.

defined, the TZ1 sandstones contain no visible cleavage, whereas the TZ2A sandstones show the onset of a penetrative cleavage. Imbricate thrust faults are inferred given the overall structure and sense of younging within the subduction complex towards the northeast (MacKinnon, 1983). These faults are difficult to resolve at the local scale, but their presence is suggested by abrupt changes in dip and a general lack of stratigraphic continuity between outcrops. We found no evidence of wide shear zones in the low textural zones within the study area. Mesocale folds are present but seem to be isolated and only locally developed in the areas we sampled.

The sampled TZ1 and TZ2A rocks come only from stratigraphically coherent sequences. Mélange zones and fold hinges were avoided. The samples are typically composed of sand-sized grains of quartz, feldspar, and volcanic-lithic clasts, with other minerals including pumpellyite, titanite, phengite and chlorite present in the matrix. In thin section, detrital quartz grains generally lack undulose extinction, subgrain boundaries, and other microstructures indicative of intragranular deformation. Quartz and feldspar grains are often truncated by mica-rich selvages, and directed overgrowths composed mainly of quartz, albite, and chlorite are common. These observations indicate that SMT was the only active ductile deformation mechanism (Norris and Bishop, 1990; Stallard and others, 2005).

We refer to the strain directions using **X**, **Y**, and **Z**, to represent the maximum stretch, intermediate, and maximum shortening directions. We cut two orthogonal sections for each sample. The first was cut parallel to cleavage, inferred to represent the **XY** plane. The average orientation of the fiber overgrowths was used to determine the **X** and **Y** directions in that plane. The second section was then cut parallel to the **XZ** plane. These principal sections show that the matrix is almost entirely made up of directed fiber overgrowths (figs. 7 and 8). The fibers are generally straight and always unidirectional, which indicates SMT deformation is constrictional or plane strain ($S_x \geq 1 \geq S_y \geq S_z$). All grain boundaries that lie at a high-angle to the fiber direction are mantled by fiber (figs. 7 and 8). In the **XZ** section, the fibers tend to parallel the trace of cleavage, which indicates that SMT deformation was coaxial (Ring and Brandon, 1999; Ring and others, 2001; Ring and Richter, 2004). Grain fracture is rarely observed and therefore inferred to be an insignificant mechanism during SMT deformation. Grain boundary sliding on planes parallel to cleavage is required to account for the heterogenous motion of diverging grains in the principal extension direction. Modal measurements (discussed below) indicate that fiber overgrowth typically makes up about 4 to 8 percent of the TZ1 and TZ2A sandstone samples we have analyzed. In

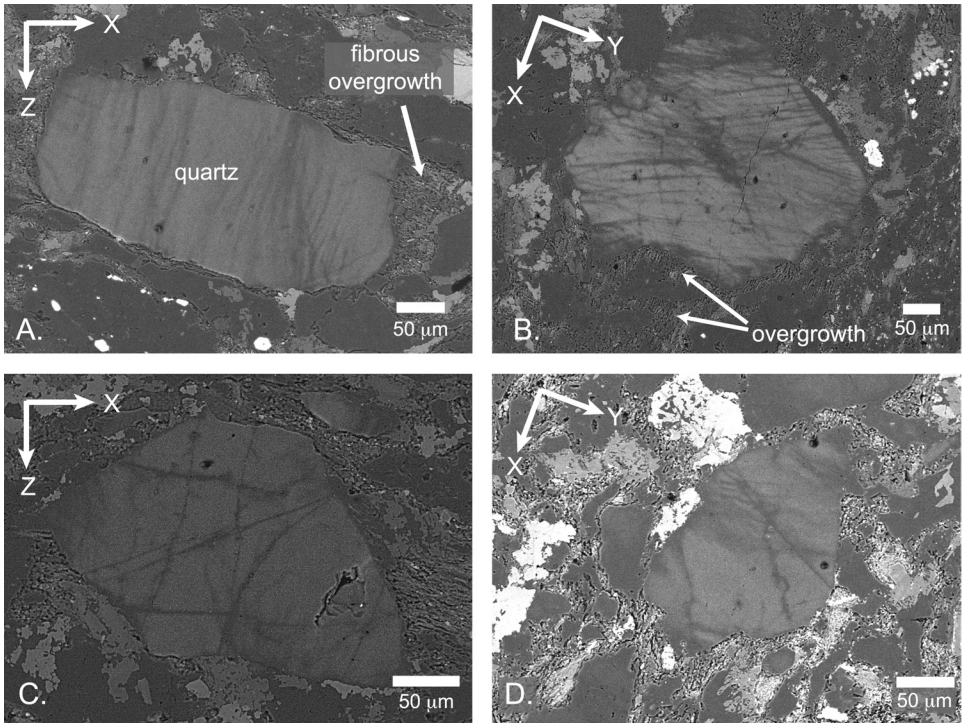


Fig. 8. Combined cathodoluminescence (CL) and electron back-scatter images (BSE) of sample 000305-5 from the Otago Schist (sample 47 from fig. 5). The large grains in the center of each image are quartz. The CL reveals internal fractures and deformation lamellae. However, these features do not have a systematic relationship to deformation features in the rock, such as the orientation of fibrous overgrowth. Thus, we interpret these features as inherited from the original source rock rather than as forming *in situ* due to deformation. The BSE portion of the image clearly shows the fibrous nature of the quartz overgrowth along the margins of many of the grains. There is no evidence of any coherent overgrowths within the quartz grains.

contrast, veins are relatively uncommon in TZ1 and TZ2A rocks. Outcrop scale measurements indicate that they comprise <3 percent of the total rock mass (Cox, 1991; Breeding and Ague, 2002). Thus, we assume that the extension in these rocks occurred primarily by formation of the fiber overgrowths.

There is a clear difference in the deformation behavior in samples from the low (TZ1 and 2a) and higher textural zones. TZ2B marks the first point where DGC begins to contribute to the ductile strain in the sandstones, with detrital quartz grains showing undulose extinction and subgrain formation. In the higher textural zones, the detrital grains and fiber overgrowths are nearly unrecognizable due to recrystallization and grain boundary migration associated with DGC (Stallard and others, 2005). Fibrous overgrowths and micaceous selvages are more abundant in TZ2B sandstones than in sandstones from lower textural zones. TZ3 marks the point where the rocks first show a segregation foliation, composed of repeating thin (several mm) quartzo-feldspathic layers, a feature widely present in the higher textural zone rocks.

Automated electron backscatter diffraction (EBSD) measurements of crystallographic preferred orientation (CPO) data of quartz grains in five metagraywacke samples were made to identify changes in active deformation mechanisms within different textural zones (see Prior and others, 1999 for a technical description of the method). The analyses were carried out with a LEO 1530 FEG scanning electron

microscope using a 20 kV acceleration voltage and a HKL EBSD detector at Bayrisches Geoinstitut, Bayreuth, Germany. Minerals and crystal orientations were indexed using the software *Channel 5* (HKL Technology Inc.). In each sample, a set of CPOs was determined by moving the electron beam over a grid of regularly spaced points. Step sizes range between 80 and 200 μm depending on the average grain size of quartz.

Samples from TZ1 and 2a show no quartz CPO. This contrasts with samples from TZ2B that show a strong preferred orientation (fig. 9). This suggests that deformation mechanisms capable of producing a CPO, such as DGC, did not operate in the low textural zone rocks. This supports our interpretation that SMT was the dominant deformation mechanism in the low-grade rocks of TZ 1 and 2A (see above). The EBSD results indicate that intracrystalline deformation is important in samples from textural zones 2B and higher, consistent with the observations of Stallard and others (2005).

As described below, our measurements of SMT strain require that 1) we account for all new precipitated material in the rocks, and 2) the detrital grains remained internally undeformed. Cathodoluminescence (CL) imaging provides a tool to identify coherent overgrowths and healed fractures in detrital grains deformed by the SMT mechanism. CL is sensitive to variations in trace element composition and thus can reveal structures that cannot be observed using standard optical methods. We studied a subset of our samples using the CL system on the JOEL JXA-8600 Electron Microprobe at Yale. The CL images do show some internal structure in the detrital quartz grains, including cracks and deformation lamellae (fig. 8). However, these features lack a preferred orientation among grains in a single section, indicating that the features were inherited from the sedimentary source for the detrital grains. We found no evidence for non-fibrous overgrowths on the detrital grains. Thus, we conclude that the fiber overgrowths were the only material to be precipitated during SMT deformation. They have clearly defined incoherent boundaries with the host grains, and thus were easy to identify for our modal measurements.

The framework of the rock consists solely of detrital grains and well-organized fiber overgrowths. The fibers show clear evidence of growth by separation and precipitation at the grain-fiber interface. The elongate quartz grains that give the overgrowths their distinctive fibrous habit are internally undeformed and the fast growth direction of the grain (parallel to the long dimension) appears to be independent of the crystallographic orientation of the grain. The overgrowths are best classified as displacement controlled antitaxial strain fringes (Passchier and Trouw, 2005, p. 175). Experimental and theoretical work has shown that this distinctive growth habit can only form when the aperture at the grain-fiber interface always remains small (several microns) relative to the average width of the fiber grains (Urai and others, 1991; Fisher and Brantley, 1992; Hilgers and others, 2001). If the aperture is large, faster growing crystal faces exposed at the grain-fiber interface tend to spread in width at the expense of the other fibers and the fibrous habit is lost. Our microscopy and CL observations indicate that all overgrowths are fibrous, which indicates that the rocks were fully compacted prior to the onset of SMT deformation.

## MEASURING SMT STRAINS

Our study of SMT deformation in the Otago wedge has focused on siliciclastic sandstones because detrital grains provide abundant strain markers (Mitra, 1976; Lisle, 1977; Mitra, 1978). One potential approach would be to estimate strains using the $R_f$-$\varphi$ method (Ramsay, 1967), but this requires that the grains deformed as passive markers. However, SMT deformation is discontinuous at the grain scale, given that deformation is accommodated by displacements at the grain boundaries and the grains themselves do not deform internally, so the grain outlines do not directly track the strain ellipse. Thus, $R_f$-$\varphi$ measurements of grain shape will not give reliable estimates of strain in pressure-solved sandstones (Lisle, 1977; Onasch, 1984). This conclusion is supported

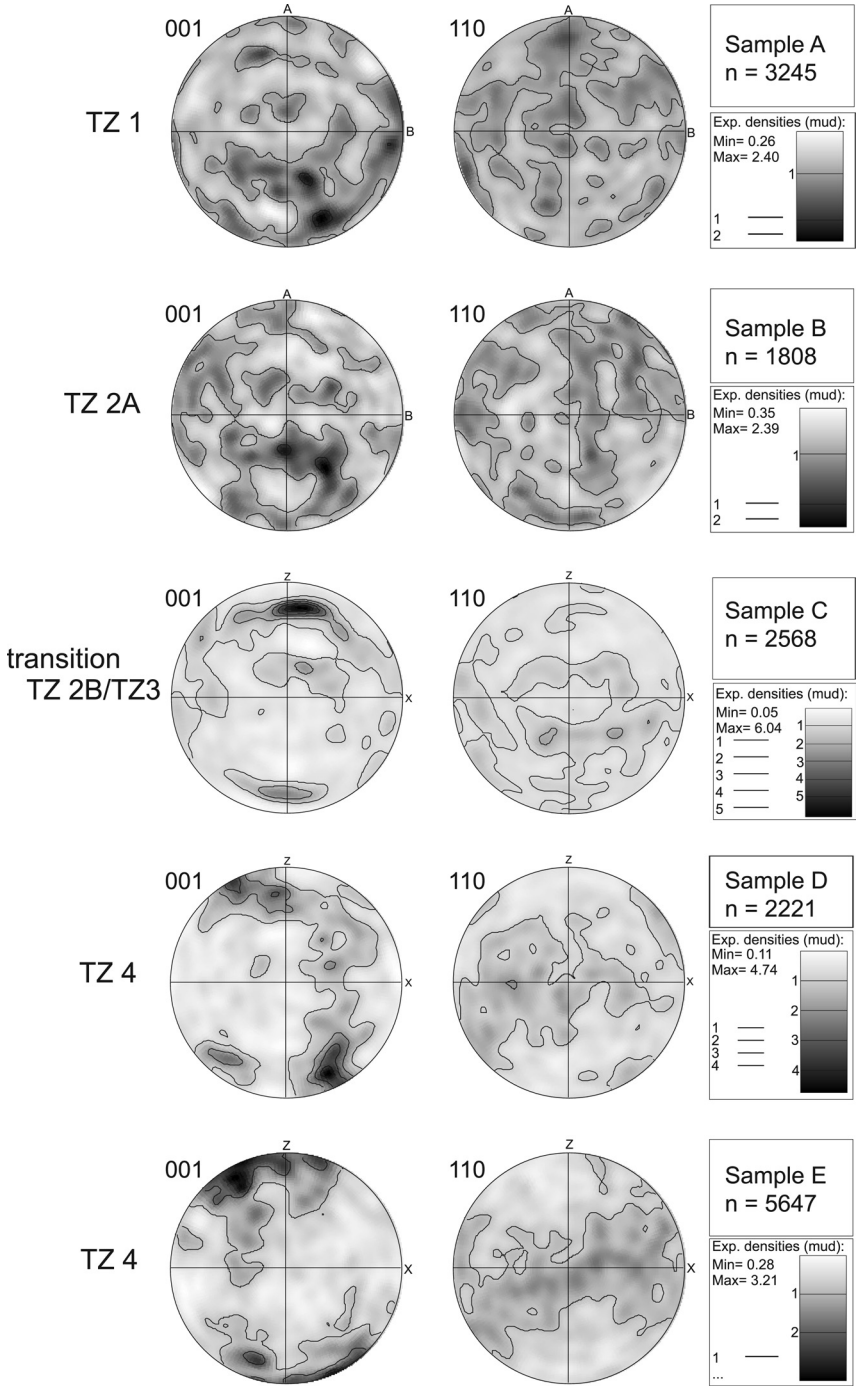


Fig. 9. Lower hemisphere, equal area stereonets showing electron back-scatter diffraction orientation data for 001 and 110 lattice directions in quartz from five samples of the Otago Schist (locations shown on fig. 5). Lower textural zone samples (TZ 1 and TZ 2A) show no lattice preferred orientation (LPO), indicating that dislocation glide was not active, which is consistent with other evidence indicating that grain-boundary pressure solution was the dominant deformation mechanism for these textural zones. In contrast, rocks from TZ 2B and higher do show quartz LPO, indicating that intracrystalline deformation has occurred.

by our own experience, which indicates that $R_f$-$\varphi$ data from pressure-solved sandstones generally fail to transform back to a random distribution when unstrained, thereby violating a fundamental requirement of the method (Shimamoto and Ikeda, 1976; Borradaile, 1984). The Fry method (Fry, 1979; Erslev and Ge, 1990) should work in principal (Onasch, 1993), but the sandstones we have studied commonly do not have a sufficiently uniform grain-size distribution to produce reliable results using this method. Furthermore, even successful application of the Fry method produces only relative, rather than absolute, strain measurements.

The PDS/Mode method of Feehan and Brandon (1999) and Ring and Brandon (1999) was specifically designed to measure absolute strains due to the SMT mechanism. The objective is to estimate the bulk SMT strain in the sample at the scale of many grains. At this scale, the material can be viewed as a continuum deforming by two processes, dissolution and precipitation. Shortening is accommodated by the growth of dissolution "selvages," which can be viewed as small "anticracks" (Fletcher and Pollard, 1981). Extension occurs by separation between grains and the growth of directed fibers in the opening voids (Williams, 1972; Mitra, 1976; Ramsay and Huber, 1983). The PDS/Mode method is based on the idea that the original grain dimension parallel to the extension direction is preserved and may be used as a marker with which to measure absolute shortening strains. The PDS/Mode method makes the following assumptions: 1) the marker grains formed a statistically isotropic fabric prior to deformation, although individual grains may have any shape. We believe this condition is generally met for sandstones in nature; 2) the initial and final dimensions of marker grains must be clearly identifiable. Intracrystalline deformation by dislocation processes, the precipitation of material within a marker grain during deformation, or the presence of unidentified overgrowth at the edge of a grain may lead to an incorrect estimate of the original grain dimension. This restricts the method to rocks in which only the SMT deformation mechanism has been active; 3) the volume of reprecipitated material should be measurable.

PDS measurements of the detrital grains were made using a petrographic microscope with camera lucida tube and an external digitizing tablet. The cursor for the tablet has a bright LED light that is projected by the camera lucida tube into the microscope field of view. Tests using a stage micrometer indicate that lengths can be measured to an accuracy of better than $\pm 3$ μm at magnifications of 100× and 250×. Measurements were made on principal sections that show one direction of shortening. We commonly observe both $S_y$ and $S_z < 1$, so for these samples measurements were made in both the **XZ** and **XY** sections.

Stretches for those principal directions that have extended ($S > 1$) are estimated using the Mode method. Since extension is accommodated through the precipitation of overgrowth, the principal extensional stretch $S_e$ in a section can be estimated from $m$, the modal fraction of fiber, using the relationship $S_e = (1 - m)^{-1}$. The modal abundance of fibers was determined by line traverses using a computer-driven micron-stepping petrographic microscope (line-integration method of Brimhall, 1979). The traverses, ~2 to 3 cm long, were measured perpendicular to the cleavage in the **XZ** section. Fibers are usually easily identified by the common directed habit of the quartz-plagioclase-mica aggregates and the relatively uniform mineralogy of the fibers across the thin section.

## RESTORATION OF PRE-ALPINE ORIENTATIONS

The rocks near the Alpine Fault show clear evidence of distributed shear to a distance of about 200 km on either side of the fault (McKenzie and Jackson, 1983; Sutherland, 1999; Hall and others, 2004). This deformation began as early as 45 Ma and probably continues at present, in association with active slip on the Alpine Fault. One concern is that this distributed shear will have rotated our strain samples, with the

degree of rotation increasing towards the Alpine Fault. To address this issue, we use the "floating block" model, in which the upper crust is viewed as a highly fractured set of small blocks that float on flowing viscous lower crust (McKenzie and Jackson, 1983). The South Island has a dense set of fission-track ages (Tippett and Kamp, 1993) that indicate that all of our samples were located at upper crustal depths (shallower than about 10 to 5 km) by about 45 Ma.

Following Sutherland (1999), we use the Maitai terrane as a reference horizon. The ophiolitic rocks of this unit have a strong magnetic signature (the Junction Magnetic anomaly) that can be easily identified even in offshore areas around New Zealand. In the Otago area, the Maitai is separated from the Otago subduction complex by the Livingstone Fault. This fault presently has a steep to overturned attitude that ensures that erosion has not significantly changed the map-view trace of the fault.

For our analysis, we assume that the shear-related displacement decreases exponentially with increasing distance normal to the Alpine Fault. Hall and others (2004) used this relationship, noting that it is the expected relationship if the lithosphere behaved like a thin viscous sheet (England and others, 1985). Like Sutherland (1999), we assume that the Maitai terrane and Livingstone Fault started with an approximately straight trend, parallel to the Otago subduction zone. These relationships are represented by

$$q(p) = q_0 + \frac{p}{\tan\theta} + A\exp\left(\frac{-p}{\lambda}\right), \tag{1}$$

where $p$ and $q$ are coordinates for points along the Livingstone Fault. The $p$-$q$ coordinate frame is defined relative to the Alpine Fault, where $p$ indicates distance normal to the Alpine fault and $q$, distance parallel to the Alpine Fault relative to an arbitrary origin along the Alpine Fault. Equation (1) has four unknown parameters: $q_0$ indicates the original position, before shearing, where the Livingstone Fault intersected the Alpine Fault; $\theta$ is the original trend of the Livingstone Fault (clockwise relative to north); $A$ is the total offset associated with distributed shearing on the Otago-side of the Alpine Fault; and $\lambda$ is the characteristic length for the exponential decay of offset away from the Alpine Fault. The parameters were estimated using least squares, where predicted values of $q$ from (1) were compared to observed values for the Livingstone Fault, as a function of $p$. The inverse is nonlinear, so it was solved using the *lsqnonlin* routine from Matlab. The equation fits the data very well, with $R^2 = 0.97$. The best-fit estimates for the parameters are: $q_0 = -56.3$ km, $\theta = 120°$, $A = 178$ km, and $\lambda = 62.7$ km. Note that this restoration only corrects for vertical axis rotations and not tilting, which is expected to be minimal throughout the Otago region.

Offset is given by

$$s = A\exp\left(\frac{-p}{\lambda}\right), \tag{2}$$

the shear by

$$\gamma = \frac{\mathrm{d}s}{\mathrm{d}p} = \frac{-p}{\lambda}A\exp\left(\frac{-p}{\lambda}\right), \tag{3}$$

and the shear-induced rotation (McKenzie and Jackson, 1983) by

$$r = \arctan\frac{\gamma}{2}. \tag{4}$$

In addition to the Alpine Fault, the Otago region is influenced by younger structures such as the Nevis or Hawkdun Faults. Slip on many distributed faults will

contribute to a deformation that appears continuous when considered at a regional scale (for example, Price, 1973). Given that our samples are collected regionally, at a scale over which mesoscopic structures such as lineations vary smoothly (Mortimer, 1993a), we can neglect the influence of local faults as we reconstruct regional ductile strain.

Figure 10 shows a restoration of the Otago wedge, with the estimated shearing associated with the Alpine Fault removed. This restoration shows a divergence of the TZ2–TZ3 boundaries as they approach the Alpine Fault. This result is expected, given the boundaries gently dip away from the Otago high and that erosion increases towards the Southern Alps and Alpine Fault.

## STRAIN RESULTS

### *Local Deformation*

Our strain results are summarized in table 1 (uncorrected sample orientations) and table 2 (orientations corrected for Alpine-related rotation). Individual samples display a wide range of strain symmetry, from prolate to oblate (fig. 11A). In general, distortional strains are small, with octahedral shear strains ($\gamma_{oct}$) $< 0.6$. The strain type is typically constrictional, with shortening in two principal directions (that is, $S_y < 1$). This holds true even for samples with oblate symmetry, creating an unusual fabric possible only because of significant volume strains (fig. 11D). Individual samples show only minor extension (<5%), despite having maximum shortening strains of ~33 percent. Volume stretch shows a good correlation with octahedral shear strain and the maximum shortening stretch (figs. 11B and 11C), indicating that distortion was accomplished primarily by the mass-transfer deformation.

Relative standard errors (RSE) were estimated using bootstrap analysis for all measurements (fig. 12). RSE[$S_x$] increases from 0 percent for $S_x \sim 1.0$ to 2.5 percent for $S_x \sim 1.23$. RSE[$S_y$] is uniform at ~8 percent, and RSE[$S_z$] increases from 4 percent for $S_z \sim 0.46$ to 8.5 percent for $S_z \sim 0.92$. The volume stretch is defined by the product $S_v = S_x S_y S_z$. RSE[$S_v$] increases from 7.3 percent for $S_v \sim 0.31$, to 12 percent for $S_v \sim 0.96$. These uncertainties include variances due to measurement errors and initial grain fabrics. Replicate measurements by trained operators give results that are within the range expected for measurement error alone.

The magnitude of deformation is similar for samples from both prowedge and retrowedge, but the orientations of the principal directions are significantly different (fig. 13). In the prowedge, **X** directions are nearly vertical, **Y** directions are widely scattered in the horizontal but generally trend SE-NW, and **Z** directions are likewise scattered in the horizontal but trend NE-SW. In the retrowedge, **X** directions are clustered around a north-trending horizontal axis, **Y** directions around an axis trending to the east with a moderate plunge, and **Z** directions around an axis trending to the west with a moderate plunge.

### *Regional Deformation*

Although strain measurements are obtained from individual rocks, our interest is at the regional scale. Observed variations in strain may stem from either local affects or large-scale heterogeneity in the deformation field. In the case of the Otago region, the uniformity of the broad structure (the Otago culmination) suggests that ductile deformation developed smoothly across the region (figs. 5 and 6). As a consequence, the main source of observed heterogeneity must be at a local scale. In a sequence of

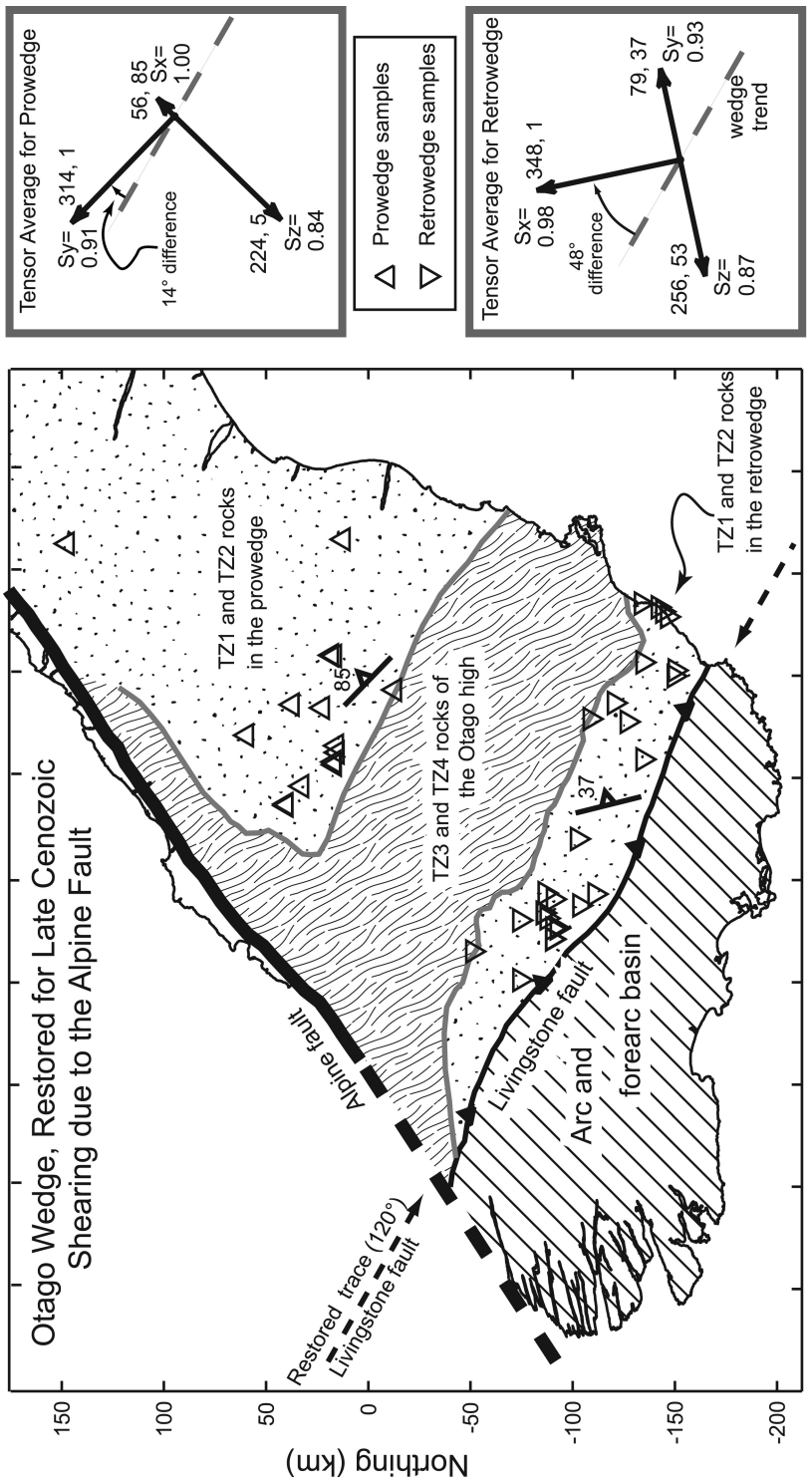


Fig. 10. Restored map of the Otago region, after removal of late Cenozoic shearing associated with the Alpine Fault (see text for details).

Table 1

*Absolute strain measurements for sandstones from the Otago subduction wedge, in current orientation*

| Map Number | Sample Number | Maximum Extension | | | Intermediate Extension | | | Maximum Shortening | | | *Sv* | New Zealand Grid Northing & Easting (m) | | Textural Zone |
|---|---|---|---|---|---|---|---|---|---|---|---|---|---|---|
| | | Trend | Plunge | *Sx* | Trend | Plunge | *Sy* | Trend | Plunge | *Sz* | | | | |
| *Retro-side of Otago high (southwest side, Caples unit)* | | | | | | | | | | | | | | |
| 1 | 0C8-3-2b | 234 | 60 | 1.10 | 331 | 5 | 1.00 | 62 | 30 | 0.62 | 0.68 | 5562100 | 2158300 | high 2A |
| 2 | 0C21-3-1 | 52 | 69 | 1.04 | 216 | 20 | 0.90 | 308 | 5 | 0.80 | 0.75 | 5534100 | 2138700 | 1 |
| 3 | AW3-1 | 355 | 76 | 1.02 | 112 | 6 | 0.96 | 203 | 12 | 0.90 | 0.89 | 5528789 | 2159828 | high 2A |
| 4 | AW-1-1 | 162 | 21 | 1.02 | 261 | 22 | 0.95 | 34 | 59 | 0.89 | 0.86 | 5510320 | 2147924 | 1 |
| 5 | AW1-2 | 159 | 8 | 1.01 | 271 | 69 | 1.00 | 66 | 19 | 0.86 | 0.87 | 5510320 | 2147924 | 1 |
| 6 | AW2-1 | 318 | 25 | 1.03 | 192 | 52 | 1.00 | 61 | 27 | 0.89 | 0.91 | 5510146 | 2148129 | 1 |
| 7 | AW2-3 | 104 | 8 | 1.02 | 11 | 22 | 0.99 | 213 | 62 | 0.88 | 0.89 | 5510146 | 2148129 | 1 |
| 8 | 0C22-3-1a | 2 | 16 | 1.05 | 92 | 2 | 0.92 | 188 | 74 | 0.92 | 0.89 | 5509400 | 2152100 | 1 |
| 9 | 0C22-3-2a | 23 | 58 | 1.01 | 194 | 31 | 1.00 | 286 | 4 | 0.75 | 0.75 | 5506800 | 2151700 | 1 |
| 10 | AW5-1 | 30 | 27 | 1.02 | 285 | 27 | 1.00 | 157 | 50 | 0.93 | 0.94 | 5512170 | 2156842 | 1 |
| 11 | AW5-2 | 12 | 27 | 1.01 | 135 | 46 | 1.00 | 264 | 31 | 0.87 | 0.88 | 5512170 | 2156842 | 1 |
| 12 | AW6-1 | 105 | 29 | 1.10 | 357 | 30 | 1.00 | 230 | 46 | 0.81 | 0.89 | 5513966 | 2159357 | 1 |
| 13 | AW6-2 | 351 | 38 | 1.07 | 151 | 50 | 0.99 | 253 | 10 | 0.85 | 0.90 | 5513966 | 2159357 | 1 |
| 14 | NZ97-3 | 324 | 53 | 1.19 | 147 | 37 | 0.96 | 56 | 2 | 0.84 | 0.96 | 5514175 | 2159445 | 1 |
| 15 | AW4-1 | 17 | 27 | 1.05 | 123 | 29 | 1.00 | 252 | 48 | 0.88 | 0.92 | 5507393 | 2163705 | 2A |
| 16 | AW4-2 | 15 | 27 | 1.06 | 149 | 54 | 1.00 | 273 | 22 | 0.87 | 0.93 | 5507393 | 2163705 | 2A |
| 17 | AW7-1 | 167 | 20 | 1.08 | 73 | 12 | 1.00 | 314 | 67 | 0.77 | 0.84 | 5511909 | 2167045 | 2A |
| 18 | AW7-3 | 158 | 9 | 1.08 | 62 | 31 | 0.97 | 262 | 57 | 0.76 | 0.79 | 5511909 | 2167045 | 2A |
| 19 | AW7-4 | 156 | 16 | 1.07 | 61 | 17 | 1.00 | 285 | 66 | 0.75 | 0.80 | 5511909 | 2167045 | 2A |
| 20 | AW7-5 | 158 | 25 | 1.05 | 253 | 10 | 1.00 | 2 | 63 | 0.72 | 0.75 | 5511909 | 2167045 | 2A |
| 21 | 2C-6 | 25 | 7 | 1.05 | 122 | 43 | 1.00 | 288 | 46 | 0.81 | 0.85 | 5492600 | 2158500 | 1 |
| 22 | 2C-1 | 65 | 36 | 1.02 | 164 | 12 | 1.00 | 270 | 51 | 0.84 | 0.85 | 5483600 | 2162000 | 1 |
| 23 | 0C19-3-1 | 20 | 33 | 1.03 | 112 | 4 | 0.93 | 209 | 57 | 0.64 | 0.61 | 5491400 | 2186900 | 2A |
| 24 | P61686 | 103 | 29 | 1.00 | 197 | 7 | 0.97 | 300 | 60 | 0.86 | 0.84 | 5455200 | 2219900 | 1 |
| 25 | 000301-1A | 17 | 17 | 1.04 | 122 | 41 | 0.98 | 268 | 44 | 0.91 | 0.93 | 5463053 | 2237720 | 2A |
| 26 | 000301-1B | 7 | 34 | 1.05 | 130 | 39 | 0.96 | 251 | 33 | 0.83 | 0.84 | 5463053 | 2237720 | 2A |
| 27 | NZ97-15 | 169 | 23 | 1.08 | 263 | 9 | 0.95 | 12 | 65 | 0.80 | 0.83 | 5469550 | 2246763 | 2B |
| 28 | 99319-6 | 333 | 50 | 1.04 | 203 | 28 | 0.98 | 98 | 26 | 0.82 | 0.84 | 5482217 | 2240011 | low 3 |
| 29 | 99320-5 | 185 | 1 | 1.04 | 93 | 61 | 0.89 | 275 | 29 | 0.88 | 0.82 | 5454820 | 2265341 | 2B |
| 30 | NZ97-16 | 51 | 46 | 1.22 | 305 | 15 | 0.98 | 202 | 40 | 0.65 | 0.78 | 5439000 | 2258500 | 1 |
| 31 | NZ97-17 | 20 | 15 | 1.05 | 190 | 75 | 0.84 | 109 | 2 | 0.68 | 0.60 | 5438600 | 2261200 | 1 |
| 32 | BB99-51 | 348 | 22 | 1.01 | 250 | 19 | 1.00 | 123 | 60 | 0.70 | 0.71 | 5442500 | 2286800 | 2A |

TABLE 1
*(continued)*

| Map Number | Sample Number | Maximum Extension | | | Intermediate Extension | | | Maximum Shortening | | | *Sv* | New Zealand Grid Northing & Easting (m) | | Textural Zone |
|---|---|---|---|---|---|---|---|---|---|---|---|---|---|---|
| | | Trend | Plunge | *Sx* | Trend | Plunge | *Sy* | Trend | Plunge | *Sz* | | | | |
| *Retro-side of Otago high (southwest side, Caples unit)* | | | | | | | | | | | | | | |
| 33 | BB99-52 | 131 | 1 | 1.02 | 41 | 40 | 0.86 | 223 | 50 | 0.66 | 0.58 | 5444900 | 2289300 | 2A |
| 34 | BB99-53 | 262 | 4 | 1.03 | 171 | 19 | 1.00 | 6 | 70 | 0.77 | 0.80 | 5447200 | 2291400 | 2A |
| 35 | Ca98-91 | 182 | 12 | 1.02 | 86 | 26 | 0.67 | 294 | 61 | 0.46 | 0.31 | 5455700 | 2293300 | high 2A |
| 36 | Ca98-92 | 186 | 25 | 1.02 | 69 | 45 | 1.00 | 295 | 35 | 0.69 | 0.70 | 5455700 | 2293300 | high 2A |
| **Tensor Average:** | | **357** | **3** | **0.98** | **89** | **37** | **0.93** | **263** | **52** | **0.87** | **0.79** | | | |
| **Flattening plane: 173, 28 E** | | | | | | | | | | | | | | |
| *Pro-side of Otago high (northeast side, Rakaia unit)* | | | | | | | | | | | | | | |
| 37 | 010309-4 | 91 | 67 | 1.05 | 320 | 16 | 1.00 | 225 | 17 | 0.79 | 0.83 | 5588233 | 2265302 | 1 |
| 38 | 000304-5 | 347 | 35 | 1.07 | 155 | 54 | 0.90 | 253 | 6 | 0.80 | 0.77 | 5610642 | 2332314 | low 2A |
| 39 | 99311-1 | 159 | 28 | 1.03 | 68 | 1 | 0.91 | 336 | 62 | 0.78 | 0.73 | 5621894 | 2286297 | 1 |
| 40 | 000307-4 | 108 | 44 | 1.01 | 15 | 3 | 0.94 | 282 | 46 | 0.90 | 0.86 | 5623708 | 2287006 | 1 |
| 41 | 99311-6 | 104 | 76 | 1.05 | 284 | 14 | 1.00 | 194 | 0 | 0.76 | 0.80 | 5634082 | 2269935 | 1 |
| 42 | LP99/20 | 305 | 76 | 1.00 | 103 | 13 | 0.88 | 194 | 5 | 0.78 | 0.69 | 5629300 | 2252200 | high 1 |
| 43 | 99312-1 | 283 | 61 | 1.03 | 21 | 4 | 0.96 | 113 | 29 | 0.89 | 0.88 | 5628955 | 2254526 | 1 |
| 44 | 0T19-2-1 | 121 | 58 | 1.00 | 298 | 32 | 0.99 | 29 | 1 | 0.53 | 0.52 | 5632800 | 2249100 | low 2A |
| 45 | 0T19-2-3 | 134 | 71 | 1.02 | 330 | 19 | 0.88 | 238 | 5 | 0.55 | 0.49 | 5632800 | 2250100 | low 2A |
| 46 | 000305-4 | 52 | 62 | 1.07 | 185 | 20 | 0.94 | 282 | 19 | 0.73 | 0.74 | 5654009 | 2277780 | 1 |
| 47 | 000305-5 | 52 | 72 | 1.06 | 176 | 10 | 0.92 | 269 | 14 | 0.74 | 0.72 | 5654009 | 2277780 | 1 |
| 48 | 000305-7 | 28 | 55 | 1.07 | 168 | 28 | 0.88 | 268 | 19 | 0.83 | 0.78 | 5654009 | 2277780 | 1 |
| 49 | 000303-1 | 345 | 70 | 1.04 | 204 | 16 | 0.88 | 111 | 12 | 0.77 | 0.70 | 5659502 | 2252845 | 1 |
| 50 | 000303-4 | 296 | 86 | 1.09 | 206 | 0 | 0.96 | 116 | 4 | 0.81 | 0.85 | 5659502 | 2252845 | 1 |
| 51 | 000304-2 | 158 | 30 | 1.05 | 338 | 60 | 1.00 | 248 | 0 | 0.89 | 0.93 | 5675419 | 2254999 | 1 |
| 52 | 000304-4 | 340 | 58 | 1.02 | 185 | 30 | 1.00 | 88 | 11 | 0.79 | 0.81 | 5675663 | 2254685 | 1 |
| 53 | NZ97-5 | 254 | 42 | 1.22 | 3 | 20 | 0.88 | 111 | 41 | 0.87 | 0.93 | 5692400 | 2284100 | 1 |
| 54 | NZ97-1 | 66 | 49 | 1.02 | 208 | 34 | 1.00 | 312 | 20 | 0.81 | 0.83 | 5796766 | 2394824 | 1 |
| **Tensor Average:** | | **59** | **85** | **1.00** | **153** | **0** | **0.90** | **243** | **5** | **0.85** | **0.76** | | | |
| **Flattening plane: 154, 85 E** | | | | | | | | | | | | | | |

TABLE 2

*Absolute strain measurements for sandstones from the Otago subduction wedge, restored for Alpine rotation*

| Map Number | Sample Number | Maximum Stretch | | | Intermediate Stretch | | | Minimum Stretch | | | *Sv* | Textural Zone |
|---|---|---|---|---|---|---|---|---|---|---|---|---|
| | | Trend* | Plunge | *Sx* | Trend* | Plunge | *Sy* | Trend* | Plunge | *Sz* | | |
| *Retrowedge samples (southwest side of Otago high, Caples unit)* | | | | | | | | | | | | |
| 1 | 0C8-3-2b | 212 | 60 | 1.10 | 309 | 5 | 1.00 | 40 | 30 | 0.62 | 0.68 | high 2A |
| 2 | 0C21-3-1 | 33 | 69 | 1.04 | 197 | 20 | 0.90 | 289 | 5 | 0.80 | 0.75 | 1 |
| 3 | AW3-1 | 341 | 76 | 1.02 | 98 | 6 | 0.96 | 189 | 12 | 0.90 | 0.89 | high 2A |
| 4 | AW-1-1 | 149 | 21 | 1.02 | 248 | 22 | 0.95 | 21 | 59 | 0.89 | 0.86 | 1 |
| 5 | AW1-2 | 146 | 8 | 1.01 | 258 | 69 | 1.00 | 53 | 19 | 0.86 | 0.87 | 1 |
| 6 | AW2-1 | 305 | 25 | 1.03 | 179 | 52 | 1.00 | 48 | 27 | 0.89 | 0.91 | 1 |
| 7 | AW2-3 | 91 | 8 | 1.02 | 358 | 22 | 0.99 | 200 | 62 | 0.88 | 0.89 | 1 |
| 8 | 0C22-3-1a | 350 | 16 | 1.05 | 80 | 2 | 0.92 | 176 | 74 | 0.92 | 0.89 | 1 |
| 9 | 0C22-3-2a | 11 | 58 | 1.01 | 182 | 31 | 1.00 | 274 | 4 | 0.75 | 0.75 | 1 |
| 10 | AW5-1 | 18 | 27 | 1.02 | 273 | 27 | 1.00 | 145 | 50 | 0.93 | 0.94 | 1 |
| 11 | AW5-2 | 0 | 27 | 1.01 | 123 | 46 | 1.00 | 252 | 31 | 0.87 | 0.88 | 1 |
| 12 | AW6-1 | 93 | 29 | 1.10 | 345 | 30 | 1.00 | 218 | 46 | 0.81 | 0.89 | 1 |
| 13 | AW6-2 | 339 | 38 | 1.07 | 139 | 50 | 0.99 | 241 | 10 | 0.85 | 0.90 | 1 |
| 14 | NZ97-3 | 312 | 53 | 1.19 | 135 | 37 | 0.96 | 44 | 2 | 0.84 | 0.96 | 1 |
| 15 | AW4-1 | 6 | 27 | 1.05 | 112 | 29 | 1.00 | 241 | 48 | 0.88 | 0.92 | 2A |
| 16 | AW4-2 | 4 | 27 | 1.06 | 138 | 54 | 1.00 | 262 | 22 | 0.87 | 0.93 | 2A |
| 17 | AW7-1 | 156 | 20 | 1.08 | 62 | 12 | 1.00 | 303 | 67 | 0.77 | 0.84 | 2A |
| 18 | AW7-3 | 147 | 9 | 1.08 | 51 | 31 | 0.97 | 251 | 57 | 0.76 | 0.79 | 2A |
| 19 | AW7-4 | 145 | 16 | 1.07 | 50 | 17 | 1.00 | 274 | 66 | 0.75 | 0.80 | 2A |
| 20 | AW7-5 | 147 | 25 | 1.05 | 242 | 10 | 1.00 | 351 | 63 | 0.72 | 0.75 | 2A |
| 21 | 2C-6 | 16 | 7 | 1.05 | 113 | 43 | 1.00 | 279 | 46 | 0.81 | 0.85 | 1 |
| 22 | 2C-1 | 57 | 36 | 1.02 | 156 | 12 | 1.00 | 262 | 51 | 0.84 | 0.85 | 1 |
| 23 | 0C19-3-1 | 13 | 33 | 1.03 | 105 | 4 | 0.93 | 202 | 57 | 0.64 | 0.61 | 2A |
| 24 | P61686 | 100 | 29 | 1.00 | 194 | 7 | 0.97 | 297 | 60 | 0.86 | 0.84 | 1 |
| 25 | 000301-1A | 14 | 17 | 1.04 | 119 | 41 | 0.98 | 265 | 44 | 0.91 | 0.93 | 2A |
| 26 | 000301-1B | 4 | 34 | 1.05 | 127 | 39 | 0.96 | 248 | 33 | 0.83 | 0.84 | 2A |
| 27 | NZ97-15 | 166 | 23 | 1.08 | 260 | 9 | 0.95 | 9 | 65 | 0.80 | 0.83 | 2B |
| 28 | 99319-6 | 329 | 50 | 1.04 | 199 | 28 | 0.98 | 94 | 26 | 0.82 | 0.84 | low 3 |
| 29 | 99320-5 | 183 | 1 | 1.04 | 91 | 61 | 0.89 | 273 | 29 | 0.88 | 0.82 | 2B |
| 30 | NZ97-16 | 49 | 46 | 1.22 | 303 | 15 | 0.98 | 200 | 40 | 0.65 | 0.78 | 1 |
| 31 | NZ97-17 | 18 | 15 | 1.05 | 188 | 75 | 0.84 | 107 | 2 | 0.68 | 0.60 | 1 |
| 32 | BB99-51 | 347 | 22 | 1.01 | 249 | 19 | 1.00 | 122 | 60 | 0.70 | 0.71 | 2A |

TABLE 2
*(continued)*

| Map Number | Sample Number | Maximum Stretch | | | Intermediate Stretch | | | Minimum Stretch | | | *Sv* | Textural Zone |
|---|---|---|---|---|---|---|---|---|---|---|---|---|
| | | Trend* | Plunge | *Sx* | Trend* | Plunge | *Sy* | Trend* | Plunge | *Sz* | | |
| *Retrowedge samples (southwest side of Otago high, Caples unit)* | | | | | | | | | | | | |
| 33 | BB99-52 | 130 | 1 | 1.02 | 40 | 40 | 0.86 | 222 | 50 | 0.66 | 0.58 | 2A |
| 34 | BB99-53 | 261 | 4 | 1.03 | 170 | 19 | 1.00 | 5 | 70 | 0.77 | 0.80 | 2A |
| 35 | Ca98-91 | 180 | 12 | 1.02 | 84 | 26 | 0.67 | 292 | 61 | 0.46 | 0.31 | high 2A |
| 36 | Ca98-92 | 184 | 25 | 1.02 | 67 | 45 | 1.00 | 293 | 35 | 0.69 | 0.70 | high 2A |
| **Tensor Average:** | | **348** | **1** | **0.98** | **79** | **37** | **0.93** | **256** | **53** | **0.87** | **0.79** | |
| (95% Confidence Interval) | | | | (0.97-1.00) | | | (0.90-0.96) | | | (0.82-0.90) | (0.74-0.84) | |
| **Flattening plane: 166, 37 E** | | | | | | | | | | | | |
| *Prowedge samples (northeast side of Otago high, Rakaia unit)* | | | | | | | | | | | | |
| 37 | 010309-4 | 80 | 67 | 1.05 | 309 | 16 | 1.00 | 214 | 17 | 0.79 | 0.83 | 1 |
| 38 | 000304-5 | 339 | 35 | 1.07 | 147 | 54 | 0.90 | 245 | 6 | 0.80 | 0.77 | low 2A |
| 39 | 99311-1 | 145 | 28 | 1.03 | 54 | 1 | 0.91 | 322 | 62 | 0.78 | 0.73 | 1 |
| 40 | 000307-4 | 94 | 44 | 1.01 | 1 | 3 | 0.94 | 268 | 46 | 0.90 | 0.86 | 1 |
| 41 | 99311-6 | 85 | 76 | 1.05 | 265 | 14 | 1.00 | 175 | 0 | 0.76 | 0.80 | 1 |
| 42 | LP99/20 | 284 | 76 | 1.00 | 82 | 13 | 0.88 | 173 | 5 | 0.78 | 0.69 | high 1 |
| 43 | 99312-1 | 263 | 61 | 1.03 | 1 | 4 | 0.96 | 93 | 29 | 0.89 | 0.88 | 1 |
| 44 | 0T19-2-1 | 99 | 58 | 1.00 | 276 | 32 | 0.99 | 7 | 1 | 0.53 | 0.52 | low 2A |
| 45 | 0T19-2-3 | 112 | 71 | 1.02 | 308 | 19 | 0.88 | 216 | 5 | 0.55 | 0.49 | low 2A |
| 46 | 000305-4 | 30 | 62 | 1.07 | 163 | 20 | 0.94 | 260 | 19 | 0.73 | 0.74 | 1 |
| 47 | 000305-5 | 30 | 72 | 1.06 | 154 | 10 | 0.92 | 247 | 14 | 0.74 | 0.72 | 1 |
| 48 | 000305-7 | 6 | 55 | 1.07 | 146 | 28 | 0.88 | 246 | 19 | 0.83 | 0.78 | 1 |
| 49 | 000303-1 | 316 | 70 | 1.04 | 175 | 16 | 0.88 | 82 | 12 | 0.77 | 0.70 | 1 |
| 50 | 000303-4 | 267 | 86 | 1.09 | 177 | 0 | 0.96 | 87 | 4 | 0.81 | 0.85 | 1 |
| 51 | 000304-2 | 124 | 30 | 1.05 | 304 | 60 | 1.00 | 214 | 0 | 0.89 | 0.93 | 1 |
| 52 | 000304-4 | 306 | 58 | 1.02 | 151 | 30 | 1.00 | 54 | 11 | 0.79 | 0.81 | 1 |
| 53 | NZ97-5 | 222 | 42 | 1.22 | 331 | 20 | 0.88 | 79 | 41 | 0.87 | 0.93 | 1 |
| 54 | NZ97-1 | 27 | 49 | 1.02 | 169 | 34 | 1.00 | 273 | 20 | 0.81 | 0.83 | 1 |
| **Tensor Average:** | | **56** | **85** | **1.00** | **314** | **1** | **0.91** | **224** | **5** | **0.84** | **0.76** | |
| (95% Confidence Interval) | | | | (0.97-1.02) | | | (0.88-0.94) | | | (0.78-0.88) | (0.70-0.81) | |
| **Flattening plane: 134, 85 N** | | | | | | | | | | | | |

* Trends corrected for shear-induced rotation associated with the Alpine fault.

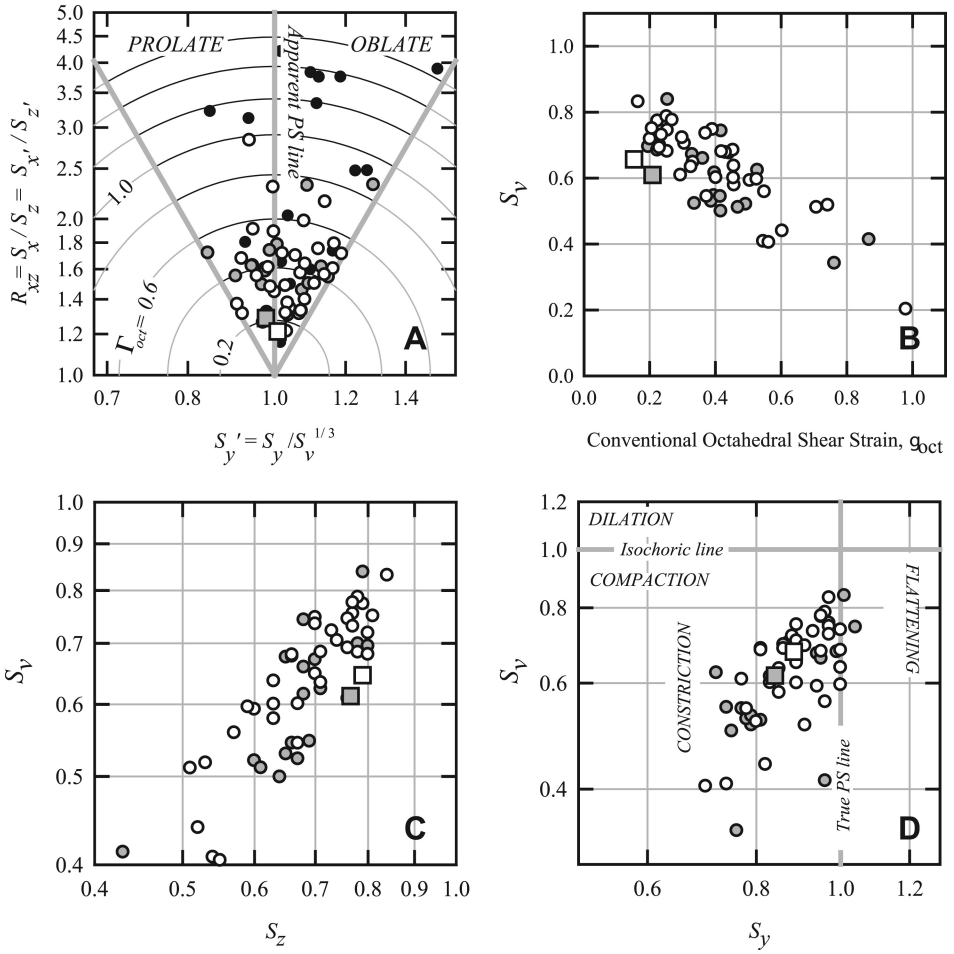


Fig. 11. Strain plots using the methods of Brandon (1995). The white and gray circles correspond to samples from the northeastern and southwestern flanks of the forearc high, respectively; black circles are data from deformed conglomerates reported in Norris and Bishop (1990). The rectangles represent the strain values for the regional tensor averages.

interbedded graywacke and mudstone like that found in the Otago region, lithologic variation causes differences in rock competence that lead to the formation of local structures. Therefore, at a minimum our average must integrate data collected at a scale larger than these lithologic variations. We also wish to increase the precision of our estimate by incorporating as many samples as possible. However, we should avoid averaging over areas where the regional structure changes greatly. Consequently, we divide our samples into two groups based on their position relative to the high-grade rocks exposed in the Otago forearc high.

Tensor averages are used here to estimate SMT strain at the regional scale. Our samples were deformed coaxially, so tensor averages can be calculated using the Hencky method of Brandon (1995). The tensor average for our sandstone samples from the prowedge indicates that $S_x$, $S_y$, $S_z$, and $S_v$ are 1.00, 0.91, 0.84, and 0.76, respectively. The flattening plane (**XY**) is nearly vertical, and has a 134° strike, sub-parallel to the 125° trend of the Otago culmination. The samples from the

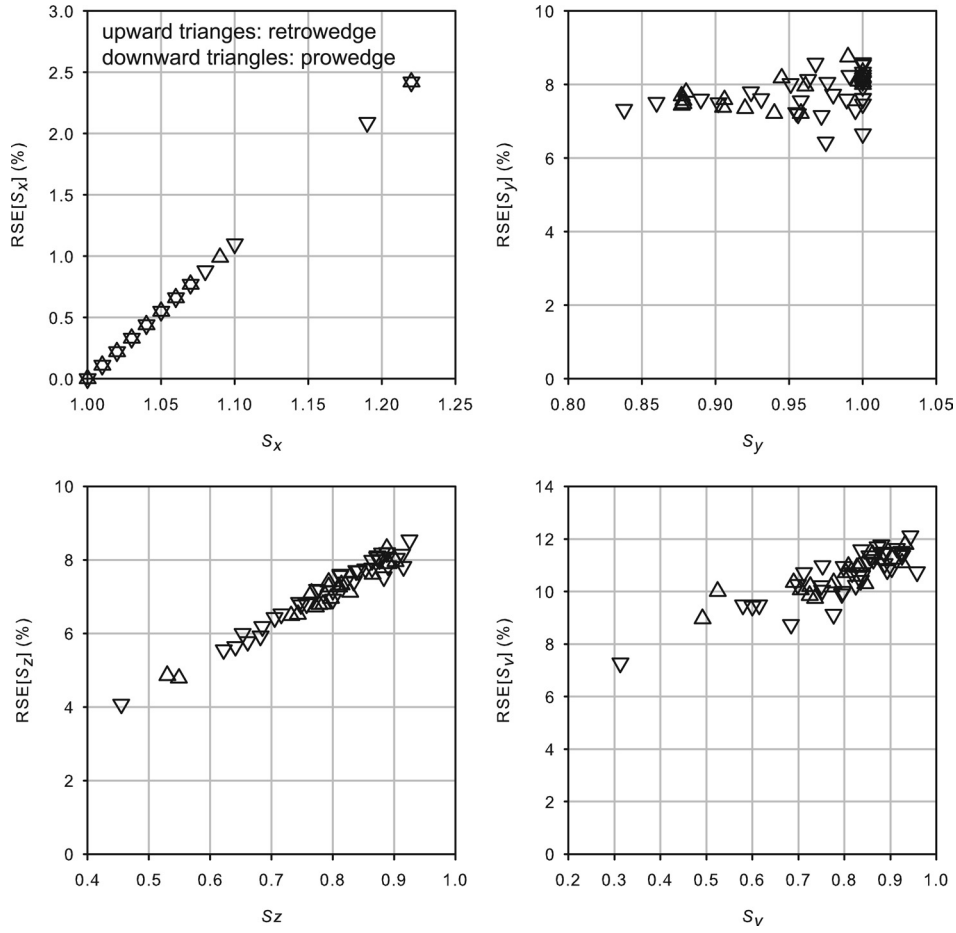


Fig. 12. Plots showing relative standard errors for principal stretch values, determined through bootstrap analysis (Efron and Tibshirani, 1994).

southwest give a tensor average with $S_x$, $S_y$, $S_z$, and $S_v$ equal to 0.98, 0.93, 0.87, and 0.79, respectively. The flattening plane strikes at 166° and dips 37° to the east. A bootstrap analysis was performed to delineate the 95 percent confidence intervals for the principal directions of the tensor averages (fig. 14).

The complete strain dataset shows significant differences in the pattern of deformation at the regional and local scales (figs. 13 and 14). The distortional strains exhibited in local samples are, in general, much greater than the bulk deformation at the regional scale. For example, the octahedral shear strain for every individual sample is greater than that for the regional tensor average (fig. 11B). On most of the strain plots, the regional tensor average falls off of the trend defined by the local strain measurements. The reason for this result is that the variance in the principal directions reduces the magnitude of the principal stretches given by the tensor averages (Brandon, 1995). In contrast, volume strain is a scalar quantity, so it can be averaged independent of the tensor values defined by the principal stretches and the principal directions.

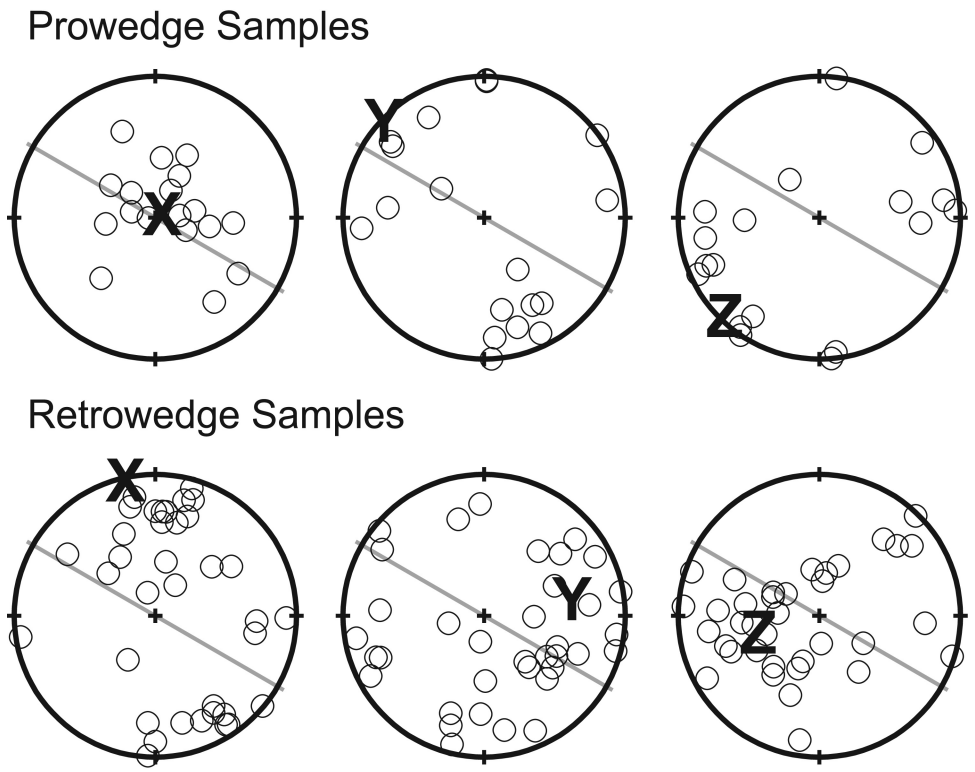


Fig. 13. Stereograms showing principal directions for each strain sample (table 2). Directions are restored for shear-related rotations associated with the Alpine Fault. X, Y, Z refer to the principal directions determined from the tensor mean. Gray line shows the modern trend of the Otago high.

## DISCUSSION

### *Deformation in the Otago Wedge*

The strain data presented here provide important new constraints on the deformational history of the Otago wedge. Although the individual measurements give insight into the local deformational field, we prefer to make tectonic interpretations using the regional tensor averages calculated for the pro- and retro-sides of the Otago wedge. Individual samples from the prowedge consistently show minor subvertical extension with shortening in one or two directions within a subhorizontal plane. The magnitude of SMT deformation is generally modest, on the order of about 5 percent extension and 10 to 45 percent shortening in the **Y** and **Z** directions (table 2). The Hencky tensor describing the regional deformation in the prowedge gives a vertically oriented flattening plane trending subparallel to the strike of the mountain belt. The magnitude of the deformation is small but consistent with a weak subvertical foliation observed in the field (for example, Mortimer, 2003).

Individual samples from the retrowedge show strains with a comparable shape and magnitude as those in the prowedge (see fig. 13). The similarity in strain intensity in the rocks of the low-grade flanks indicates that the observed deformation correlates with peak metamorphism and exhumation rather than position with respect to the toe of the wedge. Despite the similar magnitudes, there is a consistent difference in the orientation of the strain axes (fig. 14). In the southwest, the maximum stretch

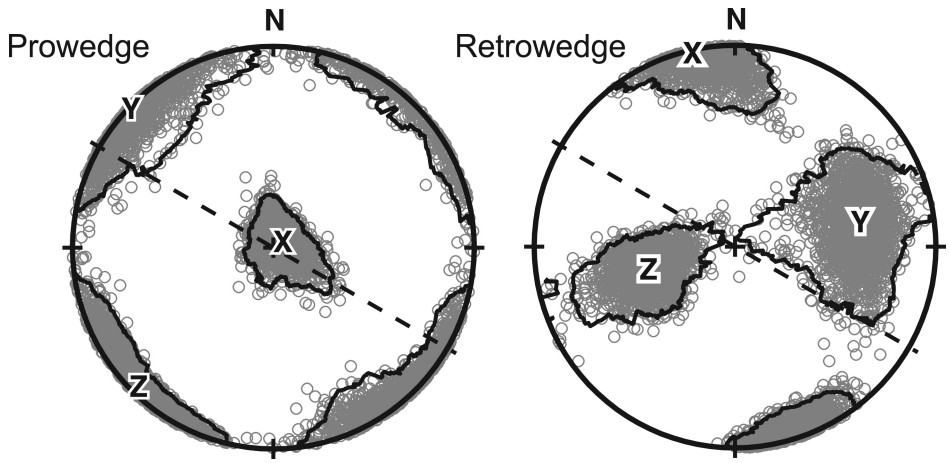


Fig. 14. Bootstrap analysis of tensor means for our strain measurements from the prowedge and retrowedge samples (table 2). The X, Y, and Z symbols mark the principal directions determined by the tensor mean. The small gray circles show the distribution of principal directions generated using bootstrap replicates for the tensor mean. These distributions are used to define the 95 percent confidence intervals (black lines) for the principal directions.

direction (**X**) is consistently sub-horizontal rather than sub-vertical. (Note that we refer to **X** as the direction of *maximum stretch* rather than *principal extension,* to avoid confusion for cases where $S_x \leq 1.0$.) Both the **Y** and **Z** axes plunge moderately in opposite directions, working together to thin the wedge in the vertical. The tensor average for the retrowedge shows that **X** has a value of about 1.0, indicating that the vertical shortening occurred without horizontal extension. The flattening plane for the deformation strikes nearly north-south and dips moderately to the east. The moderate angle (~42°) between the strike of the forearc high and trend of the **Z** axis may indicate a minor component of left-lateral rotation in the retrowedge, consistent with the proposal of Wandres and others (2004a) based on the provenance of igneous clasts within the Rakaia rocks.

The tensor averages indicate that deformation in both the pro- and retrowedge is plane-strain (that is, one of the principal stretches = 1.0). An interesting aspect to this deformation is that the plane-strain axis is not the **Y** direction but rather the maximum stretch direction (**X**). This allows the unusual circumstance of the deformation being both plane-strain and constrictional, in that two of the principal stretches are less than one. The result implies that horizontal extension has not contributed to the exhumation of the rocks in the low-grade flanks of the Otago forearc high. Rather, the observed tectonic thinning was accommodated by mass-loss.

Our strain measurements indicate spatial variations in the geometry of ductile deformation from the prowedge to retrowedge. This is consistent with the meso-scale observations of Mortimer (1993a), who noted the orientations of prominent quartz rodding lineations vary smoothly across the Otago region (fig. 6). Mortimer (1993a) interpreted these lineations to be parallel to the principal strain directions, which is confirmed by our results (figs. 6 and 14). However, the maximum stretch direction changes from subvertical in the prowedge to subhorizontal in the retrowedge (fig. 14). Although our strain analysis method is inapplicable to the higher-grade rocks exposed in the forearc high, field observations of the regional foliations (Mortimer, 1993a; Mortimer, 2003), seismic observations (Mortimer and others, 2002), and X-ray texture goniometry of mudstones (Deckert and others, 2002b) all suggest that vertical thinning is dominant in the high-grade rocks of the Otago culmination.

What might account for the change from horizontal to vertical thinning observed moving towards the rear of the wedge? We believe this transition reflects a change in the mode of accretion into the wedge. Theoretical (Dahlen, 1984), numerical (Willett, 1992), and physical models (for example, Davis and others, 1983; Lallemand and others, 1994; Gutscher and others, 1996) have shown that the velocity field within a subduction wedge reflects the material fluxes into the system. Offscraping at the front of a wedge tends to reduce wedge taper and push the system into a "sub-critical" state that promotes horizontal contraction and vertical thickening. This deformation may occur by both brittle and ductile processes and will continue until the wedge gains sufficient strength to slide stably upon its base. In contrast, parts of a wedge with an underplating flux tend to develop a gentle flattening plane, as basal accretion tends to increase wedge taper and drive vertical thinning (Platt, 1986). We note that concepts derived from two-dimensional models like those referenced here apply in settings with strike-parallel motions like Otago. A system is effectively two-dimensional if a series of cross-sections taken perpendicular to strike are similar, even if material is free to move in between the sections.

Our view of the deformation in the Otago wedge is presented in figure 15A. Accretion of incoming sediment at the toe of the system drove minor vertical thickening and the development of the weak subvertical foliation as the wedge grew to maintain a stable taper. We infer the existence of a ramp beneath the more deeply exhumed rocks of the forearc high that cut through the remainder of the incoming section and provided a significant flux of material into the wedge. Accretion likely occurred at depths of about 25 to 30 km, consistent with the published estimates of peak metamorphism in the Otago region (for example, Mortimer, 2000). The underplating caused surface uplift that pushed the forearc high above sea level, leading to subaerial erosion and terrestrial sedimentation (MacKinnon, 1983). Continued accretion lifted and pushed the structural lid back away from the prowedge, overturning the Livingstone Fault and creating the large, southwest-vergent fold of the Southland Syncline.

Similar deformation has been identified in the retro-side of many subduction wedges. For example, in Cascadia (fig. 15B), the structural lid is represented by the Crescent terrane, an oceanic unit docked to North America prior to formation of the Olympic subduction complex (Tabor and Cady, 1978). Growth of the Cascadia wedge has carried the structural lid away from the prowedge, uplifting the Crescent terrane and deforming it into a large asymmetric fold analogous to the Southland Syncline. Large-scale backfolds and steeply dipping or overturned faults are common features in the retrowedge of many orogenic systems. Other examples include the European Alps (Schmid and others, 2004), the Apennines (Fellin and others, 2007), and the Pyrenees (Muñoz, 1992).

We also compare other features of the Otago and Cascadia wedges. Although the Otago wedge is significantly wider (fig. 15), both settings are characterized by a subaerial forearc high where erosion is concentrated. Erosion rates reach similar maximum values in the high (~1.0 mm/a in Otago, 0.6-0.8 mm/a in Cascadia; Brandon and others, 1998) and drop off across strike. Yet, despite the broadly similar pattern of surface erosion, the observed deformation fabrics for the two wedges are markedly different. Although detailed strain work in the Olympics is not yet complete, Tabor and Cady (1978) have shown a steeply-dipping foliation and a consistently sub-vertical extension direction, contrasting with the structural arch observed in Otago. This example highlights the important control the mode of accretion exerts on the structural development of the wedge. In the Olympics, models of thermochronologic data (Batt and others, 2001) indicate that 80 to 100 percent of sediment was accreted frontally. As noted above, this process tends to reduce wedge taper and

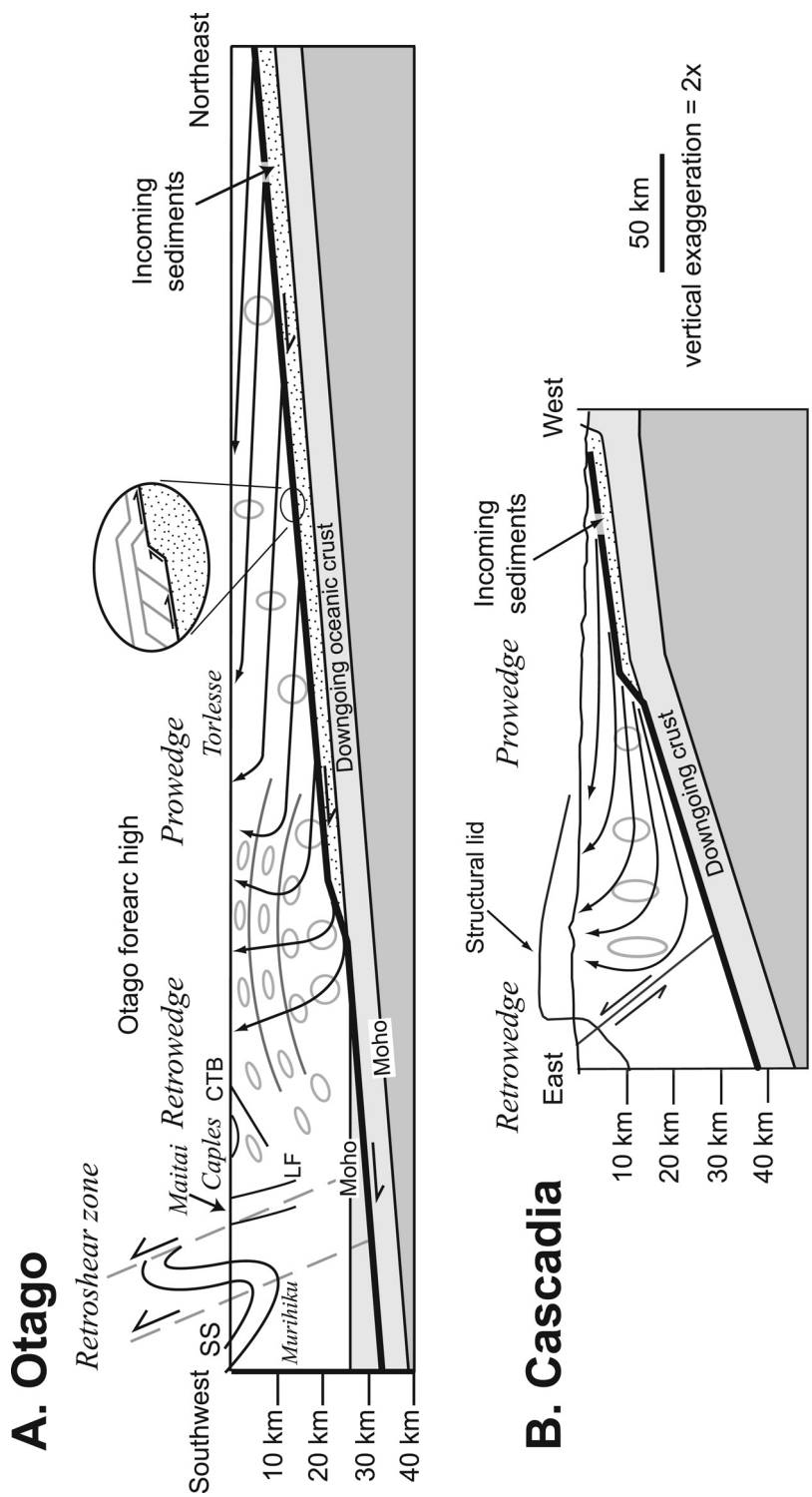


Fig. 15. (A) Cross section through the Otago wedge, schematically illustrating particle paths (black lines) and strain (light gray ellipses) through the wedge. In the front of the wedge, material is added through the scraping of sedimentary material off of the incoming oceanic crust. No extension is measured in the vertical direction, but horizontal shortening leads to the development of a weak subvertical foliation. We infer the existence of a ramp beneath the Otago forearc high that cuts through the remainder of the sedimentary cover on the incoming oceanic crust. This underplating alters the particle paths in the wedge and drives the development of a flat-lying foliation. SS—Southland Syncline; LF—Livingstone Fault; CTB—Caples/Torlesse boundary. (B) Cross section through the Cascadia wedge.

promote vertical thickening through ductile stretching and thrust faulting. Thus, despite the similar patterns of erosion, the deformational fields in the Otago and Cascadia wedges appear to be dictated by the mechanism of accretion.

### *Tectonic Coupling in Subduction Wedges*

Our observations also have implications for the strength of the boundary between the wedge and the subducting plate. Some workers have argued that deformation in the Otago region results from shearing at the base of the subducting plate (Wood, 1978; Cox, 1991). This interpretation implies a strong boundary at the base of the wedge in order to impart significant simple-shear deformation. As noted above, we argue that deformation is controlled by the distribution of accretionary and erosional fluxes around the wedge. Our observations, including the straight fibrous overgrowths and EBSD results, are consistent with a deformation that is largely coaxial. Stallard and others (2005) also reach a similar conclusion, although they do note rare σ-style overgrowths that indicate local non-coaxial deformation. Other workers have also noted local asymmetry in the region. For example, Cooper (ms, 1995) argued for simple shear deformation along the Caples-Torlesse terrane boundary based on asymmetric quartz c-axes patterns. However, in that study shear-sense indicators show a range of orientations, with some sites recording top-N shear and others showing top-S deformation. Maxelon (ms, 1999) also found asymmetric quartz c-axis fabrics in rocks from the Caples-Torlesse boundary that indicate a range of shear sense directions, including top-N and top-W. When considered together these data do not imply a consistent sense of shear. This observation illustrates that the scale of observation plays in the assessment of geologic deformation (see the *Regional deformation* section above). Because deformation at one locality may be balanced by deformation at another locality, local samples will always show deformation of a greater magnitude than what has occurred at the regional scale. In the case of the Otago wedge, the bulk deformation appears coaxial despite local examples of asymmetric shear.

The generally coaxial nature of the deformation in Otago and relatively low shear strains, both for the low-grade rocks (this study) and rocks from the core (Deckert and others, 2002b), suggests that the strength of the boundary between the downgoing plate and the Otago wedge must have been low. These findings are typical for many subduction wedges, including the Alps (Ring and others, 2001), the San Juan islands (Feehan and Brandon, 1999), the Franciscan complex (Ring and Brandon, 1999; Ring and Richter, 2004; Ring, 2008), coastal Chile (Richter and others, 2007), and Crete (Stöckhert and others, 1999; Ring and Reischmann, 2002).

### *Volume Strain*

The mass-transfer deformation in the Otago wedge displays both open and closed-system behavior on the scale of a hand sample. All samples exhibit mass-loss deformation. The average $S_v$ for the individual samples is 0.79 to 0.75, suggesting that ~20 to 25 percent of the dissolved material has been removed. This finding is consistent with results from other studies of low-grade terranes, many of which employ different approaches for estimating absolute strains (Wright and Platt, 1982; Beutner and Charles, 1985; Henderson and others, 1986; Goldstein and others, 1995, 1998; Feehan and Brandon, 1999; Ring and Brandon, 1999; Ring and others, 2001). Together, these studies suggest that significant mass-transfer volume strains may be characteristic of low-grade metamorphic terranes. Experimental studies indicate that the dihedral angles of fluids in quartz-aggregates are 60° or smaller for temperatures below 400 °C (for example, Holness, 1993). For these dihedral angles, grain boundaries will form a stable and interconnected network capable of supporting fluid flow (Bulau and others, 1979). Convergent margins are generally a fluid-rich environment and meteoric water may account for 50 to 90 percent of the fluid budget (Kastner and

others, 1991). Thus, we envision that fluid circulation within the wedge provides a mechanism to transport mass out of the Otago wedge system. Fluids flowing up-temperature are capable of dissolving silica and carrying it deeper into the wedge (Ferry and Dipple, 1991). Ultimately, these silica-rich fluids may be channeled upward and discharged into the ocean (Goldstein and others, 1998), consistent with observations of large fluid fluxes out of modern convergent wedges (Kastner and others, 1991).

## CONCLUSIONS

This paper presents a regional tectonic synthesis and a detailed study of the ductile deformation field of the Otago subduction wedge. Our work leads us to the following conclusions:

1) The Mesozoic geology of New Zealand is well-understood in the framework of a long-lived subduction wedge. In the Otago area, individual rocks preserve an integrated record of progressive deformation and metamorphism acquired during continuous advection through the wedge. The pattern of deformation and metamorphism observed today reflects the individual paths taken by the exhumed rocks rather than discrete tectonic events.
2) Significantly different views of deformation may be obtained by focusing on local versus regional deformation. Along the flanks of the Otago Schist, individual samples generally exhibit non-plane strains with extension in one principal direction and shortening in the other two principal directions. In contrast, the regional deformation is characterized by shortening in two directions, with the maximum extensional stretch generally about one. For complexly deformed terrains, care should be taken when using local observations to interpret deformation at a regional scale.
3) In the Otago prowedge, ductile deformation is characterized by horizontal shortening, with individual samples showing a weak vertical stretching. This pattern contrasts with that from the rear of the wedge, where the rocks are characterized by a shallow foliation and vertical thinning. Underplating at the base of the Otago wedge destabilized the rear of the wedge, causing a spatial transition from vertical thickening to vertical thinning. The style of deformation in wedges is controlled by the pattern of accretion.
4) Deformation within the Otago wedge is predominantly coaxial. Local observations of simple-shear have no consistent orientation and tend to balance out at a larger scale. The coaxial nature of the deformation suggests that the coupling between the downgoing plate and the overlying subduction wedge is too weak to drive simple-shear deformation in the wedge.
5) Deformation along the flanks of the forearc high was dominated by open-system pressure solution processes that led to a significant mass-loss volume stretch ($S_v = 0.75$). There are no obvious sinks for the dissolved mass, so we assume that advecting fluids have removed the dissolved material completely from the subduction wedge.

## ACKNOWLEDGMENTS

We profited from discussions with Jay Ague and Mike Breeding. Danny MacPhee provided assistance in the field and lab. We thank Florian Heidelbach from the Bayrisches Geoinstitut Bayreuth, Germany, for his introduction and assistance in the EBSD work. Anke Wohlers and Christine Kumerics provided PDS data from the Caples and Torlesse terranes, respectively, from their Diploma work at Mainz University. Matthias Bernet acquired the CL images. We thank Peter Sak and Phaedra Upton for constructive reviews. This material is based upon work supported under a National Science Foundation Graduate Research Fellowship to Rahl. This research was funded

by National Science Foundation grant EAR-9814807 to Brandon and grant Ri538/12 by the Deutsche Forschungsgemeinschaft to Ring.

## References

Adams, C. J., and Raine, J. I., 1988, Age of Cretaceous silicic volcanism at Kyeburn, Central Otago, and Palmerston, eastern Otago, South Island, New Zealand: New Zealand Journal of Geology and Geophysics, v. 31, p. 471–475.

Adams, C. J., Bishop, D. G., and Gabites, J. E., 1985, Potassium-argon studies of a low grade, progressively metamorphosed greywacke sequence, Dansey Pass, South Island, New Zealand: Journal of the Geological Society, London, v. 142, p. 339–349, doi:10.1144/gsjgs.142.2.0339.

Adams, C. J., Barley, M. E., Fletcher, I. R., and Pickard, A. L., 1998, Evidence from U-Pb zircon and $^{40}Ar/^{39}Ar$ muscovite detrital mineral ages in metasandstones for movement of the Torlesse suspect terrane around the eastern margin of Gondwanaland: Terra Nova, v. 10, p. 183–189, doi:10.1046/j.1365-3121.1998.00186.x.

Batt, G. E., and Brandon, M. T., 2002, Lateral thinking; 2-D interpretation of thermochronology in convergent orogenic settings: Tectonophysics, v. 349, p. 185–201, doi:10.1016/S0040-1951(02)00053-7.

Batt, G. E., Brandon, M. T., Farley, K. A., and Roden-Tice, M., 2001, Tectonic synthesis of the Olympic Mountains segment of the Cascadia wedge, using two-dimensional thermal and kinematic modeling of thermochronological ages: Journal of Geophysical Research, v. 106, p. 26731–26746, doi:10.1029/2001JB000288.

Beutner, E. C., and Charles, E. G., 1985, Large volume loss during cleavage formation, Hamburg Sequence, Pennsylvania: Geology, v. 13, p. 803–805, doi:10.1130/0091-7613(1985)13⟨803:LVLDCF⟩2.0.CO;2.

Bishop, D. G., 1972, Progressive metamorphism from prehnite-pumpellyite to greenschist facies in the Dansey Pass area, Otago, New Zealand: Geologic Society of America Bulletin, v. 83, p. 3177–3198, doi:10.1130/0016-7606(1972)83[3177:PMFPTG]2.0.CO;2.

——— 1994, Extent and regional deformation of the Otago peneplain: Institute of Geological and Nuclear Sciences Science Report: Lower Hutt, New Zealand, Institute of Geological & Nuclear Sciences, Report 94/1, 10, 1 sheet p.

Bishop, D. G., and Laird, M. G., 1976, Stratigraphy and depositional environment of the Kyeburn Formation (Cretaceous), a wedge of coarse terrestrial sediments in Central Otago: Journal of the Royal Society of New Zealand, v. 6, p. 55–71.

Borradaile, G. J., 1984, Strain analysis of passive elliptical markers: success of de-straining methods: Journal of Structural Geology, v. 6, p. 433–437, doi:10.1016/0191-8141(84)90044-0.

Bradshaw, J. D., 1989, Cretaceous geotectonic patterns in the New Zealand region: Tectonics, v. 8, p. 803–820, doi:10.1029/TC008i004p00803.

Brandon, M. T., 1995, Analysis of geologic strain data in strain-magnitude space: Journal of Structural Geology, v. 17, p. 1375–1385, doi:10.1016/0191-8141(95)00032-9.

——— 2004, The Cascadia subduction wedge: the role of accretion, uplift, and erosion, *in* Van der Pluijm, B., and Marshak, S., editors, Earth Structure: An Introduction to Structural Geology and Tectonics: Boston, Massachuetts, WCB/McGraw Hill Press, p. 566–574.

Brandon, M. T., Roden-Tice, M. K., and Garver, J. I., 1998, Late Cenozoic exhumation of the Cascadia accretionary wedge in the Olympic Mountains, Northwest Washington State: Geological Society of America Bulletin, v. 110, p. 985–1009, doi:10.1130/0016-7606(1998)110⟨0985:LCEOTC⟩2.3.CO;2.

Breeding, C. M., and Ague, J. J., 2002, Slab-derived fluids and quartz-vein formation in an accretionary prism, Otago Schist, New Zealand: Geology, v. 30, p. 499–502, doi:10.1130/0091-7613(2002)030⟨0499:SDFAQV⟩2.0.CO;2.

Brimhall, G. H., Jr., 1979, Lithologic determination of mass transfer mechanisms of multiple stage porphyry copper mineralization at Butte, Montana: Vein formation by hypogene leaching and enrichment of potassium-silicate protore: Economic Geology, v. 74, p. 556–589, doi:10.2113/gsecongeo.74.3.556.

Bulau, J. R., Waff, H. S., and Tyburczy, J. A., 1979, Mechanical and thermodynamical constrains on fluid distribution in partial melts: Journal of Geophysical Research, v. 84, n. B11, p. 6102–6108, doi:10.1029/JB084iB11p06102.

Burbidge, D. R., and Braun, J., 2002, Numerical models of the evolution of accretionary wedges and fold-and-thrust belts using the distinct-element method: Geophysical Journal International, v. 148, p. 542–561, doi:10.1046/j.1365-246x.2002.01579.x.

Campbell, H. J., Mortimer, N., and Raine, J. I., 2001, Geology of the Permian Kuriwao Group, Murihiku Terrane, Southland, New Zealand: New Zealand Journal of Geology and Geophysics, v. 44, p. 485–500.

Clendenen, W. S., Fisher, D., and Byrne, T., 2003, Cooling and exhumation history of the Kodiak accretionary prism, southwest Alaska, *in* Sisson, V. B., Roeske, S. M., and Pavlis, T. L., editors, Geology of a transpressional orogen developed during ridge-trench interaction along the North Pacific margin: Geological Society of America Special Papers, v. 371, p. 71–88, doi:10.1130/0-8137-2371-X.71.

Coombs, D. S., Landis, C. A., Norris, R. J., Sinton, J. M., Borns, D. J., and Craw, D., 1976, The Dun Mountain Ophiolite Belt, New Zealand, its tectonic setting, constitution and origin, with special reference to the southern portion: American Journal of Science, v. 276, p. 561–603, doi:10.2475/ajs.276.5.561.

Cooper, E. K., ms, 1995, Petrofabric studies across the Caples/Torlesse terrane boundary, Otago Schist, New Zealand: Christchurch, University of Canterbury, Msc thesis, p. 292.

Cox, S. C., 1991, The Caples/Aspiring terrane boundary; the translation surface of an early nappe structure in the Otago Schist: New Zealand Journal of Geology and Geophysics, v. 34, p. 73–82, doi:10.1080/00288306.1991.9514440.

Cox, S. C., and Barrell, D. A., 2007, Geology of the Aoraki area, Institute of Geological & Nuclear Sciences Geologic Map 15: Lower Hutt, New Zealand, GNS Science, scale 1:250,000.

Dahlen, F. A., 1984, Noncohesive critical Coulomb wedges; an exact solution, *in* Anonymous, editor, Special section; S. Thomas Crough Memorial: Journal of Geophysical Research, v. 89, n. B12, p. 10,125–10,133, doi:10.1029/JB089iB12p10125.

Davis, D., Suppe, J., and Dahlen, F. A., 1983, Mechanics of fold-and-thrust belts and accretionary wedges: Journal of Geophysical Research, v. 88, n. B2, p. 1153–1172, doi:10.1029/JB088iB02p01153.

Deckert, H., Brandon, M. T., Ring, U., Mortimer, N., and Wohlers, A., 2002b, Contribution of ductile thinning to the exhumation of the Otago Schist, New Zealand: Geological Society of America Abstracts with Programs, v. 34, p. 488.

Deckert, H., Ring, U., and Mortimer, N., 2002a, Tectonic significance of Cretaceous bivergent extensional shear zones in the Torlesse accretionary wedge, central Otago Schist, New Zealand: New Zealand Journal of Geology and Geophysics, v. 45, p. 537–547, doi:10.1080/00288306.2002.9514990.

Efron, B., and Tibshirani, R. J., 1994, An Introduction to the Bootstrap: Boca Raton, Florida, Chapman & Hall/CRC, Monographs on Statistics and Applied Probability, v. 57, 456 p.

England, P., Houseman, G. A., and Sonder, L., 1985, Length scales for continental deformation in convergent, divergent, and strike-slip environments: Analytical and approximate solutions for a thin viscous sheet model: Journal of Geophysical Research, v. 90, p. 3551–3557, doi:10.1029/JB090iB05p03551.

Erslev, E. A., and Ge, H., 1990, Quantitative fabric analysis: Least-squares center-to-center and mean object ellipse fabric analysis: Journal of Structural Geology, v. 12, p. 1047–1059, doi:10.1016/0191-8141(90)90100-D.

Feehan, J. G., and Brandon, M. T., 1999, Contribution of ductile flow to exhumation of low-temperature, high-pressure metamorphic rocks; San Juan-Cascade nappes, NW Washington State: Journal of Geophysical Research, B, Solid Earth and Planets, v. 104, p. 10,883–10,902, doi:10.1029/1998JB900054.

Fellin, M. G., Reiners, P. W., Brandon, M. T., Wüthrich, E., Balestrieri, M. L., and Molli, G., 2007, Thermochronologic evidence for the exhumational history of the Alpi Apuane metamorphic core complex, northern Apennines, Italy: Tectonics, v. 26, TC6015, doi:10.1029/2006TC002085.

Ferry, J. M., and Dipple, G. M., 1991, Fluid flow, mineral reactions, and metasomatism: Geology, v. 19, p. 211–214, doi:10.1130/0091-7613(1991)019⟨0211:FFMRAM⟩2.3.CO;2.

Fisher, D. M., and Brantley, S. L., 1992, Models of quartz overgrowth and vein formation: deformation and episodic fluid flow in an ancient subduction zone: Journal of Geophysical Research, v. 97, B13, p. 20043–20061, doi:10.1029/92JB01582.

Fletcher, R. C., and Pollard, D. D., 1981, Anticrack model for pressure solution surfaces: Geology, v. 9, p. 419–424, doi:10.1130/0091-7613(1981)9⟨419:AMFPSS⟩2.0.CO;2.

Forster, M. A., and Lister, G. S., 2003, Cretaceous metamorphic core complexes in the Otago Schist, New Zealand: Australian Journal of Earth Sciences, v. 50, p. 181–198, doi:10.1046/j.1440-0952.2003.00986.x.

Forsyth, P. J., 2001, Geology of the Waitaki area, Institute of Geological & Nuclear Sciences Geologic Map 19: Lower Hutt, New Zealand, Institute of Geological and Nuclear Sciences, GNS Science, scale 1:250,000.

Fry, N., 1979, Random point distributions and strain measurement in rocks: Tectonophysics, v. 60, p. 89–105, doi:10.1016/0040-1951(79)90135-5.

Fuller, C. W., Willett, S. D., and Brandon, M. T., 2006, Formation of forearc basins and their influence on subduction zone earthquakes: Geology, v. 34, p. 65–68, doi:10.1130/G21828.1.

Goldstein, A., Pickens, J., Klepeis, K., and Linn, F., 1995, Finite strain heterogeneity and volume loss in slates of the Taconic Allochthon, Vermont, U.S.A: Journal of Structural Geology, v. 17, p. 1207–1216, doi:10.1016/0191-8141(95)00022-6.

Goldstein, A., Knight, J., and Kimball, K., 1998, Deformed graptolites, finite strain and volume loss during cleavage formation in rocks of the taconic slate belt, New York and Vermont, U.S.A.: Journal of Structural Geology, v. 20, p. 1769–1782, doi:10.1016/S0191-8141(98)00083-2.

Gray, D. R., and Foster, D. A., 2004, $^{40}Ar/^{39}Ar$ thermochronologic constraints on deformation, metamorphism and cooling/exhumation of a Mesozoic accretionary wedge, Otago Schist, New Zealand: Tectonophysics, v. 385, p. 181–210, doi:10.1016/j.tecto.2004.05.001.

Gutscher, M. A., Kukowski, N., Malavieille, J., and Lallemand, S., 1996, Cyclical behavior of thrust wedges; insights from high basal friction sandbox experiments: Geology (Boulder), v. 24, p. 135–138, doi:10.1130/0091-7613(1996)024⟨0135:CBOTWI⟩2.3.CO;2.

——— 1998, Episodic imbricate thrusting and underthrusting; analog experiments and mechanical analysis applied to the Alaskan accretionary wedge: Journal of Geophysical Research, B, Solid Earth and Planets, v. 103, n. B5, p. 10,161–10,176, doi:10.1029/97JB03541.

Hall, L. S., Lamb, S. H., and Mac Niocaill, C., 2004, Cenozoic distributed rotational deformation, South Island, New Zealand: Tectonics, v. 23, TC2002, doi:10.1029/2002TC001421.

Haston, R. B., Luyendyk, B. P., Landis, C. A., and Coombs, D. S., 1989, Paleomagnetism and question of original location of the Permian Brook Street terrane, New Zealand: Tectonics, v. 8, p. 791–801, doi:10.1029/TC008i004p00791.

Henderson, J. R., Wright, T. O., and Henderson, M. N., 1986, A history of cleavage and folding: An example from the Goldenville Formation, Nova Scotia: Geologic Society of America Bulletin, v. 97, p. 1354–1366, doi:10.1130/0016-7606(1986)97⟨1354:AHOCAF⟩2.0.CO;2.

Hilgers, C., Koehn, D., Bons, P. D., and Urai, J. L., 2001, Development of crystal morphology during unitaxial growth in a progressively widening vein: II. Numerical simulations of the evolution of antitaxial fibrous veins, *in* White, J. C., Bleeker, W., Elliott, C., Lin, S., and van Staal Cees, R., editors, Evolution of structures in deforming rocks; in honour of Paul F. Williams: Oxford, Pergamon, Journal of Structural Geology, v. 23, p. 873–885, doi:10.1016/S0191-8141(00)00160-7.

Holness, M. B., 1993, Temperature and pressure dependence of quartz-aqueous fluid dihedral angles: the control of adsorbed $H_2O$ on the permeability of quartzites: Earth and Planetary Science Letters, v. 117, p. 363–377, doi:10.1016/0012-821X(93)90090-V.

Hutton, C. O., and Turner, F. J., 1936, Metamorphic zones in north-west Otago: Transactions of the Royal Society of New Zealand, v. 65, p. 405–406.

Jackson, J., Norris, R., and Youngson, J., 1996, The structural evolution of active fault and fold systems in central Otago, New Zealand; evidence revealed by drainage patterns, *in* Cowie, P. A., Knipe, R. J., Main, I. G., and Wojtal, S. F., editors, Special issue; Scaling laws for fault and fracture populations; analyses and applications: Journal of Structural Geology, v. 18, p. 217–234, doi:10.1016/S0191-8141(96)80046-0.

Kamp, P. J. J., 1986, Late Cretaceous–Cenozoic tectonic development of the southwest Pacific region: Tectonophysics, v. 121, p. 225–251, doi:10.1016/0040-1951(86)90045-4.

——— 2000, Thermochronology of the Torlesse accretionary complex, Wellington region, new Zealand: Journal of Geophysical Research, v. 105, p. 19253–19272, doi:10.1029/2000JB900163.

——— 2001, Possible Jurassic age for part of Rakaia Terrane; implications for tectonic development of the Torlesse accretionary prism: New Zealand Journal of Geology and Geophysics, v. 44, p. 185–203.

Kamp, P. J. J., Green, P. F., and White, S. H., 1989, Fission track analysis reveals character of collisional tectonics in New Zealand: Tectonics, v. 8, p. 169–195, doi:10.1029/TC008i002p00169.

Kastner, M., Elderfield, H., and Martin, J. B., 1991, Fluids in convergent margins: what do we know about their composition, origin, role in diagenesis and importance for oceanic chemical fluxes?: Philosophical Transactions of the Royal Society A: Physical Sciences and Engineering, v. 335, p. 243–259, doi:10.1098/rsta.1991.0045.

Kear, D., and Mortimer, N., 2003, Waipa Supergroup, New Zealand: a proposal: Journal of the Royal Society of New Zealand, v. 33, p. 149–163, doi:10.1080/03014223.2003.9517725.

Korsch, R. J., and Wellman, H. W., 1988, The geological evolution of New Zealand and the New Zealand region, *in* Nairn, A. E. M., Stehli, F. G., and Uyeda, S., editors, The Ocean Basins and Margins, v. 7B: The Pacific Ocean: New York, Plenum Press, p. 411–477.

Laird, M. G., and Bradshaw, J. D., 2004, The break-up of a long-term relationship: the Cretaceous separation of New Zealand from Gondwana: Gondwana Rsearch, v. 7, p. 273–286, doi:10.1016/S1342-937X(05)70325-7.

Lallemand, S. E., Schnuerle, P., and Malavieille, J., 1994, Coulomb theory applied to accretionary and nonaccretionary wedges; possible causes for tectonic erosion and/or frontal accretion: Journal of Geophysical Research, B6, Solid Earth and Planets, v. 99, p. 12033–12055, doi:10.1029/94JB00124.

LeMasurier, W. E., and Landis, C. A., 1996, Mantle-plume activity recorded by low-relief erosion surfaces in West Antarctica and New Zealand: Geological Society of America Bulletin, v. 108, p. 1450–1466, doi:10.1130/0016-7606(1996)108⟨1450:MPARBL⟩2.3.CO;2.

Lisle, R. J., 1977, Estimation of the tectonic strain ratio from the mean shape of deformed elliptical markers: Geologie Mijnbouw, v. 56, p. 140–144.

Little, T. A., and Mortimer, N., 2001, Rotation of ductile fabrics across the Alpine Fault and Cenozoic bending of the New Zealand Orocline: Journal of the Geological Society, London, v. 158, p. 745–756, doi:10.1144/jgs.158.5.745.

Little, T. A., Mortimer, N., and McWilliams, M., 1999, An episodic Cretaceous cooling model for the Otago-Marlborough Schist, New Zealand, based on $^{40}Ar/^{39}Ar$ white mica ages: New Zealand Journal of Geology and Geophysics, v. 42, p. 305–325.

Luyendyk, B. P., 1995, Hypothesis for Cretaceous rifting of east Gondwana caused by subducted slab capture: Geology, v. 23, p. 373–376, doi:10.1130/0091-7613(1995)023⟨0373:HFCROE⟩2.3.CO;2.

MacKinnon, T. C., 1983, Origin of the Torlesse terrane and coeval rocks, South Island, New Zealand: Geological Society of America Bulletin, v. 94, p. 967–985, doi:10.1130/0016-7606(1983)94⟨967:OOTTTA⟩2.0.CO;2.

Malavieille, J., 1984, Modelisation experimentale des chevauchements imbriques; application aux chaines de montagnes: Bulletin de la Société Géologique de France, v. 26, p. 129–138.

Massonne, H.-J., and Szpurka, Z., 1997, Thermodynamic properties of white micas on the basis of high-pressure experiments in the systems $K_2O$-MgO-$Al_2O_3$-$SiO_2$-$H_2O$ and $K_2O$-FeO-$Al_2O_3$-$SiO_2$-$H_2O$: Lithos, v. 41, p. 229–250, doi:10.1016/S0024-4937(97)82014-2.

Maxelon, M., ms, 1999, Quantification of deformation increments along the Caples-Torlesse terrane boundary, Otago, New Zealand: Mainz, Germany, University of Mainz, Dipolma Thesis, p. 86.

McKenzie, D. P., and Jackson, J. A., 1983, The relationship between strain rates, crustal thickening, palaeomagnetism, finite strain, and fault movements within a deforming zone: Earth and Planetary Science Letters, v. 65, p. 182–202, doi:10.1016/0012-821X(83)90198-X.

Miller, I. M., Brandon, M. T., and Hickey, L. J., 2006, Using leaf margin analysis to estimate the mid-Cretaceous (Albian) paleolatitude of the Baja BC block: Earth and Planetary Science Letters, v. 245, p. 95–114, doi:10.1016/j.epsl.2006.02.022.

Mitra, S., 1976, A quantitative study of deformation mechanisms and finite strain in quartzites: Contributions to Mineralogy and Petrology, v. 59, p. 203–226, doi:10.1007/BF00371309.

——— 1978, Microscopic deformation mechanisms and flow laws in quartzites within the South Mountain anticline: The Journal of Geology, v. 86, p. 129–152.

Molnar, P., Atwater, T., Mammerickx, J., and Smith, S. M., 1975, Magnetic anomalies, bathymetry and the tectonic evolution of the south Pacific since the Late Cretaceous: Geophysical Journal of the Royal Astronomical Society, v. 40, p. 383–420, doi:10.1111/j.1365-246X.1975.tb04139.x.

Mortimer, N., 1993a, Jurassic tectonic history of the Otago Schist, New Zealand: Tectonics, v. 12, p. 237–244, doi:10.1029/92TC01563.

——— 1993b, Geology of the Otago Schist and adjacent rocks: Lower Hutt, New Zealand, Institute of Geological and Nuclear Sciences Geological Map #7, Lower Hutt, New Zealand, 1 sheet p., scale 1:500,000.
——— 2000, Metamorphic discontinuities in orogenic belts: example of the garnet-biotite-albite zone in the Otago Schist, New Zealand: International Journal of Earth Sciences, v. 89, p. 295–306, doi:10.1007/s005310000086.
——— 2003, A provisional structural thickness map of the Otago Schist, New Zealand: American Journal of Science, v. 303, p. 603–621, doi:10.2475/ajs.303.7.603.
——— 2004, New Zealand's Geological Foundations: Gondwana Research, v. 7, p. 261–272, doi:10.1016/S1342-937X(05)70324-5.
Mortimer, N., and Roser, B. P., 1992, Geochemical evidence for the position of the Caples-Torlesse boundary in the Otago Schist, New Zealand: Journal of the Geological Society, London, v. 149, n. 6, p. 967–977, doi:10.1144/gsjgs.149.6.0967.
Mortimer, N., Gans, P., Calvert, A., and Walker, N., 1999a, Geology and thermochronometry of the east edge of the Median Batholith (Median Tectonic Zone); a new perspective on Permian to Cretaceous crustal growth of New Zealand: The Island Arc, v. 8, p. 404–425, doi:10.1046/j.1440-1738.1999.00249.x.
Mortimer, N., Tulloch, A. J., Spark, R. N., Walker, N. W., Ladley, E., Allibone, A., and Kimbrough, D. L., 1999b, Overview of the Median Batholith, New Zealand: a new interpretation of the geology of the Median Tectonic Zone and adjacent rocks, *in* Storey, B. C., Rubridge, B. S., Cole, D. I., and De Wit, M. J., editors, Gondwana-10; event stratigraphy of Gondwana, Proceedings, v. 1: Journal of African Earth Sciences, v. 29, p. 257–268, doi:10.1016/S0899-5362(99)00095-0.
Mortimer, N., Davey, F. J., Melhuish, A., Yu, J., and Godfrey, N. J., 2002, Geological interpretation of a deep seismic reflection profile across the Eastern Province and Median Batholith, New Zealand: crustal architecture of an extended Phanerozoic convergent orogen: New Zealand Journal of Geology and Geophysics, v. 45, p. 349–363, doi:10.1080/00288306.2002.9514978.
Muñoz, J. A., 1992, Evolution of a continental collision belt: ECORS-Pyrenees crustal balanced section, *in* McClay, K. R., editor, Thrust Tectonics: London, Chapman and Hall, p. 235–246.
Nelson, K. D., 1982, A suggestion for the origin of mesoscopic fabric in accretionary mélange, based on features observed in the Chrystalls Beach Complex, South Island, New Zealand: Geological Society of America Bulletin, v. 93, p. 625–634, doi:10.1130/0016-7606(1982)93⟨625:ASFTOO⟩2.0.CO;2.
Norris, R. J., and Bishop, D. G., 1990, Deformed conglomerates and textural zones in the Otago Schists, South Island, New Zealand: Tectonophysics, v. 174, p. 331–349, doi:10.1016/0040-1951(90)90330-B.
Onasch, C. M., 1984, Application of the Rf/[phi] technique to ellipitical markers deformed by pressure-solution: Tectonophysics, v. 110, p. 157–165, doi:10.1016/0040-1951(84)90064-7.
——— 1993, Determination of pressure solution shortening in sandstones: Tectonophysics, v. 227, p. 145–159, doi:10.1016/0040-1951(93)90092-X.
Passchier, C. W., and Trouw, R. A. J., 2005, Microtectonics: Berlin, Springer 366 p.
Platt, J. P., 1986, Dynamics of orogenic wedges and the uplift of high-pressure metamorphic rocks: Geological Society of America Bulletin, v. 97, p. 1037–1053, doi:10.1130/0016-7606(1986)97⟨1037:DOOWAT⟩2.0.CO;2.
Price, R. A., 1973, Large-scale gravitational flow of supracrustal rocks, southern Canadian Rockies, *in* De Jong, K. A., and Scholten, R., editors, Gravity and Tectonics: New York, Wiley, p. 491–502.
Prior, D. J., Boyle, A. P., Brenker, F., Cheadle, M. J., Day, A., Lopez, G., Peruzzo, L., Potts, G. J., Reddy, S. M., Spiess, R., Timms, N. E., Trimby, P. W., Wheeler, J., and Zetterstrom, L., 1999, The application of electron backscatter diffraction and orientation contrast imaging in the SEM to textural problems in rocks: American Mineralogist, v. 84, p. 1741–1759.
Rahl, J. M., Anderson, K. M., Brandon, M. T., and Fassoulas, C., 2005, Raman spectroscopic carbonaceous material thermometry of low-grade metamorphic rocks: Calibration and application to tectonic exhumation in Crete, Greece: Earth and Planetary Science Letters, v. 240, p. 339–354, doi:10.1016/j.epsl.2005.09.055.
Ramsay, J. G., 1967, Folding and fracturing of rocks: New York, McGraw-Hill, 568 p.
Ramsay, J. G., and Huber, M. I., 1983, The techniques of modern structural geology, Volume 1: Strain analysis: San Diego, California, Academic Press Inc., 309 p.
Ramsay, J. G., and Wood, D. S., 1973, The geometric effects of volume change during deformation processes: Tectonophysics, v. 16, p. 263–277, doi:10.1016/0040-1951(73)90015-2.
Reiners, P. W., and Brandon, M. T., 2006, Using thermochronology to understand orogenic erosion: Annual Reviews of Earth and Planetary Science, v. 34, p. 419–466, doi:10.1146/annurev.earth.34.031405.125202.
Richter, P. P., Ring, U., Willner, A. P., and Leiss, B., 2007, Structural contacts in subduction complexes and their tectonic significance: The Late Palaeozoic coastal accretionary wedge of central Chile: Journal of the Geological Society, v. 164, p. 203–214, doi:10.1144/0016-76492005-181.
Ring, U., 2008, Deformation and exhumation at convergent margins: The Franciscan subduction complex: Special Paper of the Geological Society of America, v. 445, p. 1–61, doi:10.1130/2008.2445.
Ring, U., and Brandon, M. T., 1999, Ductile deformation and mass loss in the Franciscan Subduction Complex—Implications for exhumation processes in accretionary wedges, *in* Ring, U., Brandon, M. T., Lister, G., and Willett, S., editors, Exhumation Processes: Normal Faulting, Ductile Flow and Erosion: Geological Society, London, Special Publications, v. 154, p. 55–86, doi:10.1144/GSL.SP.1999.154.01.03.
Ring, U., and Reischmann, T., 2002, The weak and superfast Cretan Detachment, Greece: exhumation at subduction rates in extruding wedges: Journal of the Geological Society, London, v. 159, p. 225–228, doi:10.1144/0016-764901-150.
Ring, U., and Richter, P. P., 2004, Normal faulting at convergent plate boundaries: The Del Puerto Canyon shear zone in the Franciscan subduction complex revisited: Tectonics, v. 23, C2006, doi:10.1029/2002TC001476.

Ring, U., Brandon, M. T., Willett, S. D., and Lister, G. S., 1999, Exhumation processes, *in* Ring, U., Brandon, M. T., Lister, G. S., and Willett, S. D., editors, Exhumation processes; normal faulting, ductile flow and erosion: Geological Society, London, Special Publications, v. 154, p. 1–27, doi:10.1144/GSL.SP.1999.154.01.01.

Ring, U., Brandon, M. T., and Ramthun, A., 2001, Solution-mass-transfer deformation adjacent to the Glarus Thrust, with implications for the tectonic evolution of the Alpine wedge in eastern Switzerland: Journal of Structural Geology, v. 23, p. 1491–1505, doi:10.1016/S0191-8141(01)00015-3.

Schmid, S. M., Fügenschuh, B., Kissling, E., and Schuster, R., 2004, TRANSMED Transect IV, V and VI: Three lithospheric transects across the Alps and their forelands, *in* Cavazza, W., Roure, F., Spakman, W., Stampfli, G. M., and Ziegler, P. A., editors, The TRANSMED Atlas: The Mediterranean Region from Crust to Mantle: Berlin, Heidelberg, New York, Springer Verlag.

Shimamoto, T., and Ikeda, Y., 1976, A simple algebraic method for strain estimation from deformed ellipsoidal objects. 1. Basic Theory: Tectonophysics, v. 36, p. 315–337, doi:10.1016/0040-1951(76)90107-4.

Stallard, A., and Shelley, D., 2005, The initiation and development of metamorphic foliation in the Otago Schist, Part 1: competitive oriented growth of white mica: Journal of Metamorphic Geology, v. 23, p. 425–442, doi:10.1111/j.1525-1314.2005.00587.x.

Stallard, A., Shelley, D., and Reddy, S., 2005, The initiation and development of metamorphic foliation in the Otago Schist, Part 2: evidence from quartz grain-shape data: Journal of Metamorphic Geology, v. 23, p. 443–459, doi:10.1111/j.1525-1314.2005.00590.x.

Stöckhert, B., Wachmann, M., Küster, M., and Bimmermann, S., 1999, Low effective viscosity during high pressure metamorphism due to dissolution precipitation creep; the record of HP-LT metamorphic carbonates and siliclastic rocks from Crete: Tectonophysics, v. 303, p. 299–319, doi:10.1016/S0040-1951(98)00262-5.

Sutherland, R., 1999, Cenozoic bending of New Zealand basement terranes and Alpine Fault displacement: a brief review: New Zealand Journal of Geology and Geophysics, v. 42, p. 295–301, doi:10.1080/00288306.1999.9514846.

Sutherland, R., and Hollis, C., 2001, Cretaceous demise of the Moa plate and strike-slip motion at the Gondwana margin: Geology, v. 29, p. 279–282, doi:10.1130/0091-7613(2001)029⟨0279:CDOTMP⟩2.0.CO;2.

Tabor, R. W., and Cady, W. M., 1978, The structure of the Olympic Mountains, Washington—analysis of a subduction zone: United States Geological Survey, Professional Paper 1033, p. 38.

Tippett, J. M., and Kamp, P. J. J., 1993, Fission track analysis of the late Cenozoic vertical kinematics of continental Pacific crust, South Island, New Zealand: Journal of Geophysical Research, n. B9, Solid Earth and Planets, v. 98, p. 16119–16148, doi:10.1029/92JB02115.

Tulloch, A. J., Ramezani, J., Mortimer, N., Mortensen, J., van den Bogaard, P., and Maas, R., 2009, Cretaceous felsic volcanism in New Zealand and Lord Howe Rise (Zealandia) as a precursor to final Gondwana break-up, *in* Ring, U., and Wernicke, B., editors, Extending a Continent: Architecture, Rheology and Heat Budget: Geological Society, London, Special Publications, v. 321, p. 89–118, doi:10.1144/SP321.5.

Turnbull, I. M., Mortimer, N., and Craw, D., 2001, Textural zones in the Haast Schist; a reappraisal: New Zealand Journal of Geology and Geophysics, v. 44, p. 171–183, doi:10.1080/00288306.2001.9514933.

Urai, J. L., Williams, P. F., and van Roermund, H. L. M., 1991, Kinematics of crystal growth in syntectonic fibrous veins: Journal of Structural Geology, v. 13, p. 823–836, doi:10.1016/0191-8141(91)90007-6.

Vry, J. K., Baker, J., Maas, R., Little, T. A., Grapes, R., and Dixon, M., 2004, Zoned (Cretaceous and Cenozoic) garnet and the timing of high grade metamorphism, Southern Alps, New Zealand: Journal of Metamorphic Geology, v. 22, p. 137–157, doi:10.1111/j.1525-1314.2004.00504.x.

Vry, J. K., Powell, R., and Williams, J., 2008, Establishing the *P-T* path for Alpine Schist, Southern Alps near Hokitika, New Zealand: Journal of Metamorphic Geology, v. 26, p. 81–97, doi:10.1111/j.1525-1314.2007.00746.x.

Wandres, A. M., Bradshaw, J. D., Weaver, S., Maas, R., Ireland, T., and Eby, N., 2004a, Provenance of the sedimentary Rakaia sub-terrane, Torlesse Terrane, South Island, New Zealand: the use of igneous clast compositions to define the source: Sedimentary Geology, v. 168, p. 193–226, doi:10.1016/j.sedgeo.2004.03.003.

——— 2004b, Provenance analysis using conglomerate clast lithologies: a case study from the Pahau terrane of New Zealand: Sedimentary Geology, v. 167, p. 57–89, doi:10.1016/j.sedgeo.2004.02.002.

Willett, S. D., 1992, Dynamic and kinematic growth and change of a Coulomb wedge, *in* McClay, K., editor, Thrust Tectonics: New York, Chapman and Hall, p. 19–31.

Willett, S. D., and Brandon, M. T., 2002, On steady states in mountain belts: Geology, v. 30, p. 175–178, doi:10.1130/0091-7613(2002)030⟨0175:OSSIMB⟩2.0.CO;2.

Willett, S., Beaumont, C., and Fullsack, P., 1993, Mechanical model for the tectonics of doubly vergent compressional orogens: Geology, v. 21, p. 371–374, doi:10.1130/0091-7613(1993)021⟨0371:MMFTTO⟩2.3.CO;2.

Williams, P. F., 1972, Development of metamorphic layering and cleavage in low-grade metamorphic rocks at Bermagui, Australia: American Journal of Science, v. 272, p. 1–47, doi:10.2475/ajs.272.1.1.

Wood, B. L., 1978, The Otago schist megaculmination: its possible origins and tectonic significance in the Rangitata orogen of New Zealand: Tectonophysics, v. 47, p. 339–368, doi:10.1016/0040-1951(78)90038-0.

Wright, T. O., and Henderson, J. R., 1992, Volume loss during cleavage formation in the Meguma Group, Nova Scotia, Canada: Journal of Structural Geology, v. 14, p. 281–290, doi:10.1016/0191-8141(92)90086-C.

Wright, T. O., and Platt, L. B., 1982, Pressure dissolution and cleavage in the Martinsburg shale: American Journal of Science, v. 282, p. 122–135, doi:10.2475/ajs.282.2.122.